Effect of Tetra-*m*-bromo and Tetra-*m*-methyl Buttressing on the Ground-State Structures, Rotational Barriers, and Keto⇌Enol Equilibria of 2,2-Dimesityl-1-R-ethenols[1]

Irina Eventova, Ella B. Nadler, Elimelech Rochlin, Joseph Frey, and Zvi Rappoport*

Contribution from the Department of Organic Chemistry, The Hebrew University of Jerusalem, Jerusalem 91904, Israel. *Received June 23, 1992. Revised Manuscript Received November 12, 1992*

Abstract: The stable enols $(3,5\text{-}Br_2\text{-}2,4,6\text{-}Me_3C_6)_2C{=}C(OH)R$ (**3a–d**) and $(Me_5C_6)_2C{=}C(OH)R$ (**9a–d**), R = H, Me, Mes, or *t*-Bu, were prepared. The effect of buttressing by four *m*-Br or *m*-Me groups was investigated by comparison with the 2,2-dimesityl analogs $Mes_2C{=}C(OH)R$ (**1**). No buttressing effect on the ease of formation of **3** and **9** was observed. Differences due to buttressing in torsional and bond angles in the solid-state structures were mostly moderate or small, the largest being when R = H. The threshold rotational mechanisms for **1**, **3**, and **9** are a one-ring flip when R = H, a two-ring flip when R = Me or *t*-Bu, and a three-ring flip when R = Mes. The one-ring flip barrier is higher for **3a** and **9a** than for **1a** due to increased buttressing in the transition state for the rotation. The two- and three-ring-flip barriers are lower for **3** and **9** than for **1**. These differences are partially accounted for by solvent effects and by electronic and torsional angle effects on the extent of ground-state Ar—C=C conjugation for most of the enols but not when R = *t*-Bu. Enols **3a** and **3d** do not isomerize to the keto–enol mixtures even after prolonged heating in hexane/CF_3COOH. This is ascribed to increased kinetic stability over enols **1** due to reduced nucleophilicity by the electron-withdrawing bromines. Enols **9a**, **9b**, and **9d** and the isomeric ketones of **9b** and **9d** isomerize in hexane/CF_3COOH at 80 °C to the equilibrium mixtures. The higher K_{enol} values of 185 (**9a**), 3.6 (**9b**), and 0.021 (**9d**) compared to those for the corresponding enols **1**, were attributed to increased crowding. In conclusion, after accounting for electronic effects, the buttressing effect by four *m*-Br or *m*-Me groups on the solid-state structures, rotational barriers, and keto ⇌ enol equilibria is mostly moderate.

The presence of bulky aromatic substituents and Ar—C=C conjugation are the major effects which enable isolation of stable aryl-substituted enols and affect their properties.[2] Steric effects in these systems affect structural, thermodynamic, and dynamic phenomena. For example, the increased steric bulk of R in 2,2-dimesityl-1-R-ethenols (**1**) from H to *t*-Bu results in appreciably

$Mes_2C{=}C(OH)R$	$Mes_2CHC(=O)R$
1a: R = H	**2a**: R = H
1b: R = Me	**2b**: R = Me
1c: R = Mes	**2c**: R = Mes
1d: R = *t*-Bu	**2d**: R = *t*-Bu

Mes = Mesityl

increased bond angles R—C=C and Ar—C=C torsional angles.[3a] These angles are higher for **1c** than for **1a** but lower for **1c** than for **1d**.[3b] Both the mechanism of internal rotation around the mesityl—C=C bond and the rotational barriers depend on the bulk of R. The mesityl rings always rotate in a correlated rotation, and the lowest energy (threshold) rotational mechanism is a one-ring flip for **1a**, a two-ring flip when R = alkyl, e.g., for **1b**,[4] and a three-ring flip for **1c**.[5] The two-ring-flip barriers $\Delta G_c^{\ddagger}$ decreases from 14.2 kcal mol^{-1} for **1a** to 10.4 kcal mol^{-1} for **1d**[4] and are linearly correlated with Taft's E_s values[2b,4b,6] and the Ar—C=C torsional angles.[2b,4b] Consequently, the higher the ground-state torsional angle, the less energy is required to rotate the mesityl group to the ideal two-ring-flip transition state having orthogonal Mes and C=C moieties.

The keto ⇌ enol equilibrium constants for **2** ⇌ **1** (K_{enol}) in hexane decrease from 20 for **1a** to 0.006 for **1d**,[6,7] and $\Delta G°(R)$ values for the **1** ⇌ **2** equilibria are linear with E_s.[6] However, for **1c**, K_{enol} = 79,[7a] whereas it is 1.0 when R = Ph,[7b] reflecting increased K_{enol} with the increased bulk of a 1-aryl substituent. Likewise, K_{enol} decreases on decreasing the bulk of one β-aryl group from mesityl to phenyl.[7a,c]

Consequently, it is interesting how a further increase in the bulk of the β-aryl groups will affect the synthesis of these bulky enols, their solid-state structures, their rotational mechanisms and barriers, and the keto ⇌ enol equilibria. We increased the bulk of the β-aryl groups by replacing the mesityl groups with 2,4,6-triisopropylphenyl groups[8] and by buttressing the *o*-Me groups by four meta substituents of moderate bulk.

Buttressing was first applied for biphenyls and related systems[9] and was recently applied in order to obtain carboxylic acid enols.[10] Oki had shown an inverse buttressing effect on rotational barriers of triptycenes,[11] and the effect of 4,5-substituents on structures and rotations in phenanthrenes was also reported.[12] Buttressing by *m*-bromo substituents did not affect much the ground-state structure of dimesitylketene.[13]

(1) (a) Stable Simple Enols. 33. Part 32: Swahn, L.; Ahlberg, P.; Rappoport, Z. *Croat. Chem. Acta* **1992**, *65*, 745. (b) Preliminary reports: Nadler, E. B.; Eventova, I.; Rappoport, Z. 10th IUPAC Conference on Physical Organic Chemistry, Haifa, Israel, August 5–10, 1990; Abstract p 124. Eventova, I.; Nadler, E. B.; Rappoport, Z. 3rd European Symposium on Organic Reactivity, Goteborg, Sweden, July 7–12, 1991; Abstract p 83.

(2) (a) For a review on isolable and relatively stable enols see Hart, H.; Rappoport, Z.; Biali, S. E. In *The Chemistry of Enols*; Rappoport, Z., Ed.; Wiley: Chichester, U.K., 1990; Chapter 8, pp 481–590. (b) Rappoport, Z.; Biali, S. E. *Acc. Chem. Res.* **1988**, *21*, 442.

(3) (a) Kaftory, M.; Nugiel, D. A.; Biali, S. E.; Rappoport, Z. *J. Am. Chem. Soc.* **1989**, *111*, 8181. (b) Kaftory, M.; Biali, S. E.; Rappoport, Z. *J. Am. Chem. Soc.* **1985**, *107*, 1701.

(4) (a) Nugiel, D. A.; Biali, S. E.; Rappoport, Z. *J. Am. Chem. Soc.* **1984**, *106*, 3357. (b) Biali, S. E.; Nugiel, D. A.; Rappoport, Z. *J. Am. Chem. Soc.* **1989**, *111*, 846.

(5) Biali, S. E.; Rappoport, Z. *J. Am. Chem. Soc.* **1984**, *106*, 477.

(6) Nugiel, D. A.; Rappoport, Z. *J. Am. Chem. Soc.* **1985**, *107*, 3669.

(7) (a) Biali, S. E.; Rappoport, Z. *J. Am. Chem. Soc.* **1985**, *107*, 1007. (b) Nadler, E. B.; Rappoport, Z. *J. Am. Chem. Soc.* **1987**, *105*, 2112. (c) Rappoport, Z.; Biali, S. E. *Bull. Soc. Chim. Belg.* **1982**, *91*, 388.

(8) Frey, J.; Rappoport, Z. (a) Unpublished results; (b) 57th Meeting of the Israel Chemical Society, Haifa, Israel, February 12–13, 1992; Abstract L-32.

(9) (a) Rieger, M.; Westheimer, F. H. *J. Am. Chem. Soc.* **1950**, *72*, 19. (b) Chein, S. L.; Adams, R. *J. Am. Chem. Soc.* **1934**, *56*, 1787. (c) Westheimer, F. H. In *Steric Effects in Organic Chemistry*; Newman, M. S., Ed.; Wiley: New York, 1956; Chapter 12, p 552.

(10) O'Neill, P.; Hegarty, A. F. *J. Chem. Soc., Chem. Commun.* **1987**, 744.

(11) (a) Yamamoto, G.; Suzuki, M.; Oki, M. *Bull. Chem. Soc. Jpn.* **1983**, *56*, 809. (b) Oki, M. *Top. Stereochem.* **1983**, *14*, 1.

(12) Armstrong, R. N.; Ammon, H. L.; Darnow, J. N. *J. Am. Chem. Soc.* **1987**, *109*, 2077.

(13) Biali, S. E.; Gozin, M.; Rappoport, Z. *J. Phys. Org. Chem.* **1989**, *2*, 271.

0002-7863/93/1515-1290$04.00/0

We report here the effects of substituting enols **1a–d** with four *m*-bromo substituents or four *m*-methyl substituents on the crystallographic structure, on the rings' rotation, and partially on the keto ⇌ enol equilibria.

Results

Synthesis. Enols **3a–c** were prepared from reaction of tetrabromodimesitylketene (**5**) with $LiAlH_4$, MeLi, or MesMgBr, respectively (eq 1). We were unable to obtain the 1-*t*-Bu de-

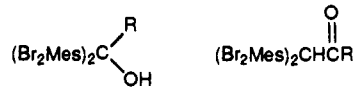

3a: R = H
3b: R = Me
3c: R = Mes
3d: R = *t*-Bu

4a: R = H
4b: R = Me
4c: R = Mes
4d: R = *t*-Bu

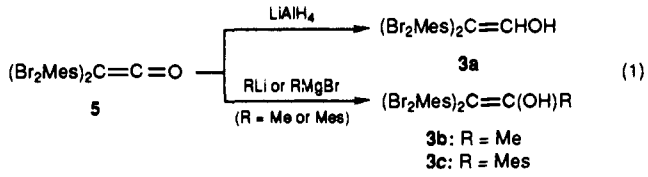

3b: R = Me
3c: R = Mes

(1)

rivative **3d** by reaction of 1.3–3 molar equiv of *t*-BuLi with **5** in ether or THF. The reaction gave a complex mixture of products showing signals for aromatic hydrogens in the ^1H NMR and of less than four bromines in the mass spectra, indicating that a main reaction is lithium/bromine exchange. The products were not investigated further.

In an alternative approach, enol **1d** was reacted with bromine. Depending on the amount of bromine, a mixture of products, containing brominated ketones and benzofurans[14] but no brominated derivative of **1d**, was formed. This reaction will be described elsewhere.

Enol **3d** was finally obtained by bromination of **6**, the acetate of enol **1d**, followed by reduction of the formed acetate **7** to the enolate, which was then protonated (eq 2).

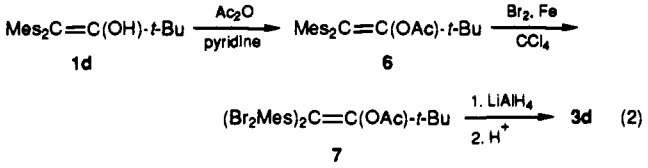

(2)

The isopropyl ether of **3a**, i.e. **8**, was prepared by a phase-transfer alkylation of **3a** (eq 3).

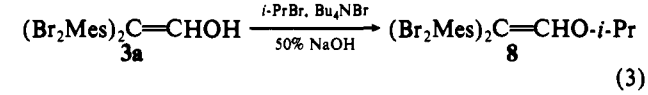

(3)

Four 2,2-bis(pentamethylphenyl)-1-R-ethenols **9a–d** were also prepared by reacting ketene **10**[15] with $LiAlH_4$, MeLi, MesLi, and *t*-BuLi, respectively (eq 4).

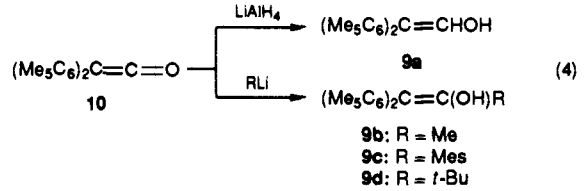

9b: R = Me
9c: R = Mes
9d: R = *t*-Bu

(4)

Ketones **11b** and **11c** were isolated from equilibration of their isomeric enols **9b** and **9d**, respectively, in hexane/CF_3COOH at

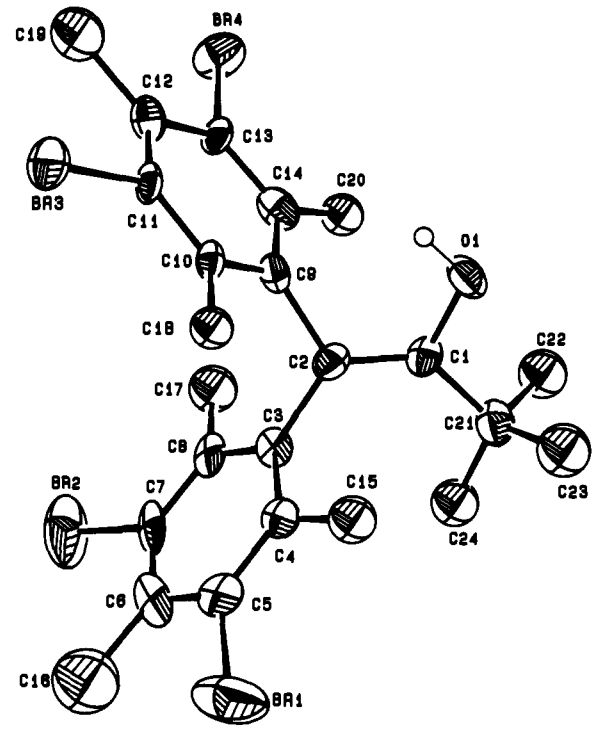

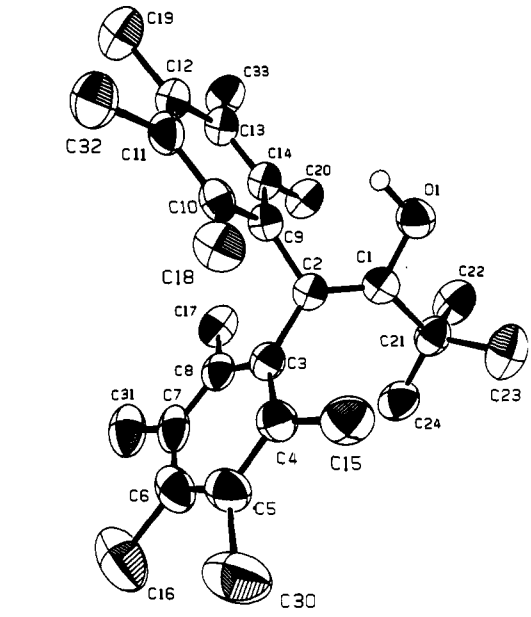

Figure 1. ORTEP drawings and numbering scheme for enols (a, top) **3d** and (b, bottom) **9d**.

80 °C (eq 5). **11a**, which is formed only in ca. 0.5% in the corresponding equilibria, was not isolated.

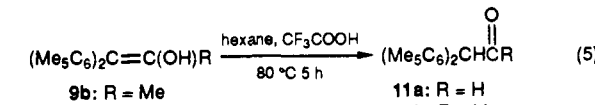

9b: R = Me
9d: R = *t*-Bu

11a: R = H
11b: R = Me
11c: R = *t*-Bu

(5)

Solid-State Structures. The solid-state structures of enols **3a–d**, **9a**, and **9d** were determined by X-ray crystallography. Most enols crystallize with a solvent of crystallization: **3a** and **3b** with ether, **3c** with MeOH, and **9a** with CH_2Cl_2, and only the 1-*tert*-butyl enols crystallize without a solvent of crystallization. The numbering schemes for **3d** and **9d** are shown in their ORTEP structures in Figure 1. The numbering is similar for **3a** and **9a**, with H1 replacing C21–C24, for **3b** with H atoms instead of C22–C24, and for **3c**, where C21–C26 are the ring carbons, C27 and C29 are the *o*-Me carbons, and C28 is the *p*-Me carbon of the 1-mesityl

(14) Oxidation of crowded stable enols to benzofurans is a known reaction: (a) Bailey, P. S.; Potts, F. E., III; Ward, J. W. *J. Am. Chem. Soc.* **1970**, *92*, 230. Bailey, P. S.; Ward, J.-W.; Potts, F. E., III; Chang, Y.-G.; Hornish, R. E. *J. Am. Chem. Soc.* **1974**, *96*, 7228. (b) Schmittel, M.; Baumann, U. *Angew. Chem., Int. Ed. Engl.* **1990**, *29*, 541.

(15) Clarke, L. F.; Hegarty, F. A.; O'Neill, P. *J. Org. Chem.* **1992**, *57*, 362. Clarke, L. F.; Hegarty, A. F. *J. Org. Chem.* **1992**, *57*, 1940.

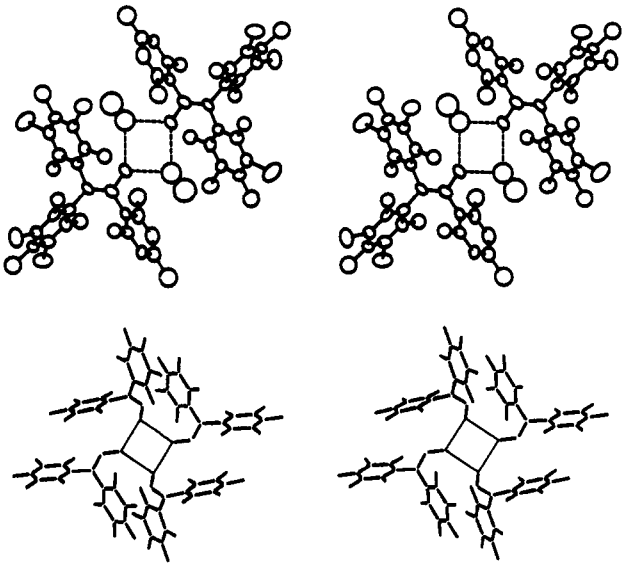

Figure 2. Hydrogen bonding in solid enols: (a, top) 3c·MeOH; (b, bottom) 9a.

ring. The other ORTEP drawings, the stereoscopic views, and the unit cell drawings for several enols are given in Supplementary Figures S1–S9.

Two types of hydrogen bonding are shown in Figure 2, where the OH hydrogens (not shown) are between two oxygen atoms. In the solvate 3c·MeOH the hydrogen-bonding array involves a cyclic alternating arrangement of two molecules each of 3c and MeOH (Figure 2a). In 9a four molecules are bonded as a cyclic tetramer (Figure 2b) and the solvating CH_2Cl_2 is not hydrogen bonded to the OH. An anti arrangement of the C=C—OH moiety with intermolecular hydrogen bonding to a solvating ether molecule is observed for 3b, whereas the 1-*tert*-butyl enols 3d and 9d show no intramolecular enol–enol association and an OH syn to the *cis*-aryl group.

As found previously,[3] the Ar_2C moiety in all the enols studied here has a propeller conformation. The two rings (or the three rings of 3c) are twisted in the same sense in relation to the double bond.

Selected bond lengths are given in Table I and selected bond angles in Table II. The complete list of bond lengths and angles and positional, thermal, and structural parameters is given in Supplementary Tables S1–S30. With 3a, the vinylic hydrogen was not accurately located, so that α_4 and α_5 are not given. The Ar—C=C torsional angles (Table III) are 55.9–63.1°. With enols 3a, 9a, and 9b the Ar—C=C torsional angle of the ring trans to OH is lower than that for the ring cis to the OH, whereas for 3b–d both angles are almost the same. These angles increase with the increased bulk of the 1-substituent. The double-bond torsional angles are relatively small, except when R = *t*-Bu, when they are 14° and 15°.

As found for the nonbrominated compounds 1a–d,[3] the bond angles change regularly with the increased bulk of R. The largest change is the opening of the R—C=C angles to 132.4° for 3d and 132.8° for 9d. Table IV gives the difference in degrees in the bond and torsional angles between 3 and 9 and the corresponding *m*-H enols (1) as $\Delta^{31} = \angle(3) - \angle(1)$ and $\Delta^{91} = \angle(9) - \angle(1)$. Angles α_1–α_6, ϕ_1, and ϕ_2 are defined in Figure 3. The differences are mostly small, the larger ones being $\Delta\phi_2$ for the α-H derivatives. Interestingly, the Δ's of the most crowded α-*tert*-butyl derivatives are negative. Differences in the bond angles are also small, some being negative. The torsional angles of the double bond itself in 1, 3, and 9 are similar; the Δ's are 2° and 1°, respectively.

No appreciable effect of the *m*-Br or *m*-Me substituents on the bond angles involving the *o*-Me substituents was observed. The $C_{ipso}C_oC_{Me}$ and $C_mC_oC_{Me}$ angles are 122.4 ± 0.4° and 122.3 ± 0.2° for 3 and 121.2 ± 0.2° and 120.1 ± 0.1° for 9. The rings are essentially planar; the average deviation of ring atoms from the average ring plane is 0.0045–0.0163 Å for the rings in the seven structures. The deviation is always smaller for the ring cis to the OH.

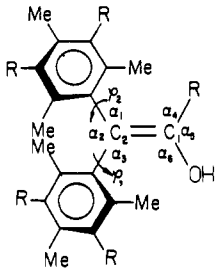

Figure 3. Designations of angles for 2,2-diarylethenols.

Static NMR Spectra. Rotation of the aryl groups at room temperature of most of the enols is fast on the NMR time scale. The static NMR spectra of the 2,2-diarylethenols and the ether 8 in 3:7 CS_2/CD_2Cl_2 (Table V) were determined below the coalescence temperature, and those of the triarylethenols 3c and 9c were determined at room temperature in $C_6D_5NO_2$ (Table VI).

The static spectra of enols 3 and 9 resemble those of enols 1. The two very close highest field methyl signals are those for *o*-Me groups in the β- and β'-rings. The other two *o*-Me groups are at a much lower field. $\Delta\delta$ values between *o*-Me groups in each ring are 0.50–0.86 ppm. For the *p*-Me groups in the two rings $\Delta\delta$ = 0–0.03 ppm. All the methyls, especially the *p*-Me signals of the tetrabromo enols 3, are downfield shifted compared with those in enols 1. In contrast, the shifts of the *o*-Me and *p*-Me values in the tetra-*m*-Me enols 9a–c are remarkably similar to those in 1. The $\Delta\delta$(*m*-Me) values in enols 9 on each ring are much smaller than the $\Delta\delta$(*o*-Me) values.

The α-mesityl ring of enols 1c, 3c, and 9c in $C_6D_5NO_2$ influences the differences discussed above. However, the similarities in the spectra of 1c and 9c in $C_6D_5NO_2$ at 295 K can still assist in a tentative signal assignment in the more complex spectrum of 9c (Table VI).

Rotation of the Aryl Rings. Dynamic NMR Studies. Table V gives the ^1H NMR spectrum of enols 1a, 1b, 3a, 3b, 3d, 9a, 9b, and 9d and of the isopropyl ether 8 at 266.5–315 K in 3:7 CS_2/CD_2Cl_2. For these systems, the *o*-Me signals of the rings appear as sharp or broad singlets in reduced number compared with the low-temperature spectra, indicating that coalescence of the *o*-Me signals due to rotation of the rings already took place. On cooling the solutions in 3:7 CS_2/CD_2Cl_2, the *o*-Me signals of each ring and the *m*-Me signals of 9a and 9b broaden and decoalesce, and each appears as a singlet (except for accidental isochronicity) below the coalescence temperatures (Table VII), in line with a frozen propeller conformation. Pairs of coalescing signals were mostly identified by the saturation transfer technique and sometimes by analogy. The use of 3:7 CS_2/CD_2Cl_2 v/v is due to its low freezing temperature and to solubility considerations at the low temperature. On raising the temperature, coalescence was observed and the rotational barriers $\Delta G_c^{\#}$ were calculated by using the Gutowsky–Holm approximation[16] and the Eyring equation. For 3b, 3d, and 9b the two barriers calculated from coalescence of the two *o*-Me groups of each ring were identical within the experimental errors. The $\Delta\nu$ values below the coalescence temperature T_c, the T_c values, and the $\Delta G_c^{\#}$ values are given in Table VII together with the values for enols 1.[4]

The α-alkyl and *p*-Me signals shifted on changing the temperature but remained sharp. The OH signal shifted to a lower field at the lower temperatures, as was previously observed.[17]

The coalescence study of enols 9 was more complicated due to the presence of ≥10 methyl signals in a narrow δ range, which led to several accidental isochronicities. The *m*-Me coalescence processes were also followed, but extensive overlap and shift of the signals with the temperature result in somewhat less accurate derived $\Delta G_c^{\#}$ values.

(16) Gutowsky, H. S.; Holm, C. H. *J. Chem. Phys.* **1956**, *25*, 1228.
(17) Rochlin, E.; Rappoport, Z. *J. Am. Chem. Soc.* **1992**, *114*, 230.

Table I. Selected Bond Lengths (in Å) for Six 2,2-Bis(pentasubstituted-phenyl)-1-R-ethenols

bond	3a[a]	3b[a]	3c[b]	3d	9a[c] A	9a[c] B	9d
C1–C2	1.32 (1)	1.35 (2)	1.34 (2)	1.35 (1)	1.325 (4)	1.328 (5)	1.345 (4)
C1–O	1.32 (1)	1.39 (2)	1.36 (1)	1.37 (1)	1.365 (4)	1.365 (4)	1.392 (4)
C2–C3	1.52 (1)	1.49 (2)	1.52 (1)	1.54 (1)	1.518 (4)	1.498 (5)	1.520 (4)
C2–C9	1.529 (8)	1.53 (2)	1.49 (2)	1.51 (1)	1.509 (4)	1.507 (4)	1.521 (4)
C1–C21		1.49 (2)	1.50 (2)	1.54 (1)			1.524 (4)
5Ar(C–C)[d]	1.38 (9)–1.41 (1)	1.37 (2)–1.40 (2)	1.36 (2)–1.41 (2)[e]	1.37 (2)–1.41 (1)	1.387 (5)–1.406 (5)	1.389 (5)–1.417 (5)	1.383 (5)–1.409 (4)
C3–C8	1.44 (1)	1.43 (2)	1.41 (2)	1.42 (1)	1.397 (4)	1.407 (4)	1.404 (4)
4 Ar(C–C)[f]	1.39 (1)–1.42 (1)	1.38 (3)–1.42 (2)	1.36 (2)–1.40 (2)[g]	1.39 (1)–1.42 (1)	1.391 (4)–1.405 (4)	1.398 (5)–1.413 (5)	1.386 (4)–1.429 (4)
C10–C11	1.357 (5)	1.38 (2)	1.37 (2)	1.40 (1)	1.405 (4)	1.398 (5)	1.407 (4)
C13–C14	1.364 (9)	1.37 (2)	1.37 (2)	1.42 (1)	1.391 (4)	1.409 (5)	1.524 (4)
C–Me[h]	1.48 (1)–1.56 (1)[i]	1.48 (2)–1.53 (3)[i]	1.48 (2)–1.51 (2)	1.48 (1)–1.51 (2)	1.502 (5)–1.525 (5)[k]	1.494 (5)–1.518 (6)	1.501 (4)–1.536 (5)[l]
C–Br[m]	1.88 (7)–1.91 (7)	1.90 (2)–1.93 (2)	1.89 (1)–1.91 (1)	1.897 (8)–1.94 (1)			

[a] 3-Et_2O. [b] 3c·MeOH. [c] Crystallizes with 0.5 molecules of CH_2Cl_2 in two crystallographically different molecules (A and B) in the unit cell. [d] In ring trans to OH. [e] C4–C5, C12–C13: 1.36 (2) Å. [f] In ring cis to OH. [g] For the 1-mesityl ring: 6Ar(C–C), 1.36 (2)–1.40 (2) Å; 3 C–Me, 1.49 (2)–1.52 (2) Å. [h] Six bonds in 3; 10 bonds in 9. [i] C6–C16, 1.56 (1) Å. All the other five bonds are 1.48 (1)–1.53 (1) Å. [j] C12–C19, 1.53 (3) Å. [k] Longer bonds C14–C20 (A), C6–C16 (B) 1.525 Å; shorter bonds C8–C17 (B) 1.494 Å, C4–C15 (B) 1.496 Å. [l] Average: 1.515 ± 0.006 Å. The longer bond is C5–C30 1.536 (5) Å. The shorter bond is C10–C18 1.501 Å. [m] 4 C–Br bonds.

Table II. Selected Bond Angles (in deg) for Six 2,2-Bis(pentasubstituted-phenyl)-1-R-ethenols

angle	3a[a]	3b[a]	3c[b]	3d	9a[c] A	9a[c] B	9d
O1C1C2	127.1 (9)	118 (1)	117 (1)	119.4 (8)	123.1 (3)	123.5 (3)	119.5 (3)
C1C2C3	117.4 (7)	121.1 (1)	123 (1)	124.7 (8)	117.7 (3)	118.0 (3)	126.2 (3)
C1C2C9	122.2 (6)	120 (1)	120 (1)	119.6 (7)	120.4 (3)	120.0 (3)	118.5 (3)
C3C2C9	120.3 (5)	119 (1)	117 (1)	115.7 (7)	121.8 (2)	122.0 (3)	115.2 (2)
C2C1C21		126 (1)	130 (1)	132.4 (8)			132.8 (3)
O1C1C21		116 (1)	113 (1)	107.8 (7)			107.5 (2)
4 $C2C_{ipso}C_o$	118.0 (6)–122.0 (7)	118 (1)–121 (1)	118.8 (9)–122 (1)	118.6 (8)–120.6 (8)	119.7 (3)–121.1 (3)	119.5 (3)–121.1 (3)	120.1 (2)–121.3 (2)
3 $C_mC_oC_{ipso}$ + 2 $C_oC_{ipso}C_o$	118.4 (6)–120.5 (6) (av 119.2)	116 (1)–122 (1) (av 119)	115 (1)–119 (1)[j] (av 117.8)	117.0 (9)–120.5 (8) (av 118.6)	119.1 (3)–120.8 (3) (av 119.9 ± 0.6)	118.7 (3)–120.6 (3) (av 119.5 ± 0.6)	118.4 (3)–120.6 (3) (av 119.5 ± 0.8)
4 $C_oC_mC_p$	122.5 (8)–124.5 (7) (av 123.8)	123 (1)–126 (1) (av 124.3)	123 (1)–126 (1) (av 124.5)	124.2 (8)–126 (1) (av 125.3)	119.8 (3)–120.3 (3) (av 120.0 ± 0.2)	119.5–121.0 (av 120.6 ± 0.4)	119.8 (3)–121.1 (av 120.5 ± 0.5)
2 $C_mC_pC_m$	115.1 (8), 115.8 (6)	115 (1), 116 (1)	116 (2), 119 (1)	114 (1), 115.0 (9)	119.9 (3), 120.0 (3)	119.5 (3), 120.4 (3)	119.6 (3), 119.7 (3)
C3C8C7	116.8 (6)	117 (1)	119 (1)	116.7 (9)	120.4 (3)	120.8 (3)	120.8 (3)
4 $C_{ipso}C_oC_{Me}$	121.2 (8)–123.2 (6) (av 122.2)	122 (1)–124 (1) (av 122.8)	121 (1)–123 (1)[g] (av 121.8)	120.0 (8)–124.1 (8) (av 122.2)	118.7 (3)–121.7 (3)[h] (av 121.4 ± 0.03)	119.3 (3)–123.1 (3)[h] (av 121.4 ± 0.13)	119.0 (3)–122.4 (3) (av 120.9 ± 0.12)
4 $C_mC_oC_{Me}$	118.4 (6)–121.4 (7) (av 119.5)	116 (1)–121 (1) (av 119)	119 (1)–121 (1) (av 120.3)	118.2 (7)–123.2 (9) (av 120.6)	118.0 (3)–120.4 (3) (av 118.8 ± 0.08)	118.2 (3)–120.5 (3) (av 118.3 ± 0.12)	117.7 (3)–121.2 (3) (av 119.5 ± 0.12)
4 $C_mC_pC_{Me}$	121.6 (7)–123.3 (8) (av 122.3)	120 (1)–123 (1) (av 122)	120 (2)–125 (1) (av 122.5)	121.9 (8)–123.1 (8) (av 122.5)	119.3 (3)–120.3 (4) (av 120.0 ± 0.05)	119.1 (4)–121.2 (4) (av 120.0 ± 0.08)	119.3 (3)–121.0 (3) (av 120.2 ± 0.07)
4 C–C–Br[d]	117.5 (6)–118.3 (5) (av 118.0)	117 (1)–120 (1) (av 118.3)	116 (1)–120 (1) (av 117.8)	116.7 (8)–117.7 (7) (av 117.2)			
4 C–C–Br[e]	116.6 (6)–120.9 (6) (av 118.3)	116 (1)–118 (1) (av 117.3)	117.1 (9)–118.0 (9) (av 117.7)	116.5 (7)–118.5 (7) (av 117.7)			
4 $C_pC_mC_{Me}$					119.2 (3)–120.6 (3) (av 119.8 ± 0.05)	118.7 (4)–120.5 (3) (av 119.7 ± 0.08)	119.3 (3)–120.5 (3) (av 119.7 ± 0.04)
4 $C_oC_mC_{Me}$					119.6 (3)–120.6 (3) (av 120.1 ± 0.03)	119.1 (3)–120.9 (3) (av 120.2 ± 0.05)	119.3 (3)–120.5 (3) (av 120.0 ± 0.05)

[a] 3-Et_2O. [b] 3c·MeOH. [c] Crystallizes with 0.5 molecules of CH_2Cl_2 in two crystallographically different molecules (A and B) in the unit cell. [d] In ring trans to OH. [e] In ring cis to OH. [f] For the 1-ring the six inter-ring angles are 119 (2)–121 (2)°. [g] For the 1-ring $C_{ipso}C_oC_{Me}$ 122°, 123°. [h] C3C4C15 ≥ 121.7°.

Table III. Torsional Angles for 2,2-Bis(hexasubstituted-phenyl)ethenols[a]

torsional angle	3a	3b	3c	3d	9a A	9a B	9d
C=C	3.7	7.0	6.0	15.1	2.8	3.9	14.2
C_β-Ar(1) (ϕ_1)[b]	55.9	61.0	59.8	61.4	59.1	60.3	60.1
C_β-Ar(2) (ϕ_2)[b]	58.6	60.7	59.5	61.7	54.9	58.9	63.1
Ar(1)-Ar(2)[b]	90.1	86.2	91.6	95.9	92.9	85.7	92.7
C_α-Ar(α)			56.0				
Ar(α)-Ar(1)[b]			69.8				
Ar(α)-Ar(2)[b]			59.3				

[a] C_α = O1C1C21 or O1C1H1; C_β = C3C2C9. [b] Ar(1) = ring cis to OH; Ar(2) = ring trans to OH.

Table IV. Differences in Torsional and Bond Angles between Enols 3 or 9 and 1[a]

difference	Δ^{31}[b] α-H	α-Me	α-Mes	α-t-Bu	Δ^{91}[c] α-H	α-t-Bu
$\Delta\phi_1$	−0.8	3.5	7.8	−4.6	3.0	−5.9
$\Delta\phi_2$	8.4	5.3	3.1	−2.0	6.7	−0.7
$\Delta\phi_3$[d]			2.1			
$\Delta\alpha_1$	−0.7	−0.8	−1.0	−0.7	−0.2	0.8
$\Delta\alpha_2$	−0.7	0.8	−1.4	−0.6	0.9	−1.3
$\Delta\alpha_3$	1.9	0.1	0.5	1.3	0.4	0.2
$\Delta\alpha_4$		0	0.4	−0.8		−0.4
$\Delta\alpha_5$		3.6	3.5	0.4		0.1
$\Delta\alpha_6$	3.4	−3.6	−3.8	0.2	−0.4	0.3

[a] The average of the angles was taken when there was more than one crystallographically independent molecule in the unit cell. [b] $\Delta^{31} = \angle(3) - \angle(1)$. [c] $\Delta^{91} = \angle(9) - \angle(1)$. [d] Torsional angle of the α-Ar group with the C=C bond.

For example, for **9b**, the sharp signals at 1.67 and 2.19 ppm at 165 K, which are at δ 1.70 and δ 2.19, 2.20, respectively, at 295 K, were assigned to the α-Me and *p*-Me groups. A two methyl signal at 1.63 ppm at 165 K is ascribed to two isochronous *o*-Me groups on two rings. Both coalesce with the two *o*-Me signals at δ 2.33 and 2.35 at T_c = 221.4 K, giving $\Delta G^\#$ = 10.0 ± 0.1 kcal mol^{-1} for both processes. At 295 K the *o*-Me groups display a four-methyl broadened singlet. Two 2 H *m*-Me signals each at δ 2.04 and 2.23 at 165 K undergo coalescence at 205.5 K, giving $\Delta G_c^\#$ = 9.8 ± 0.1 kcal mol^{-1}, and display two sharp singlets at δ 2.14 and 2.15, at 295 K.

Enol **3d** displays at 292 K two sharp *o*-Me singlets at δ 2.26 and 2.32, which give a single decoalescence temperature at 180 K, $\Delta G_c^\#$ = 8.2 kcal mol^{-1}. At 167.6 K, the *o*-Me signals are still broad, each appearing as an overlap of two signals, so that $\Delta\nu$ below T_c and T_c are less accurate (estimated error ±0.3 kcal mol^{-1}) than for other enols. The δ(*o*-Me) at 292 K are not at the average position of the low temperature values probably due to a slight shift of the signals with the temperature.

The OH, the CH, and the *o*- and *p*-Me signals of **1a**, **3a**, and **9a** undergo low-temperature changes which are ascribed to formation of intermolecular enol–enol hydrogen bonding. This behavior will be reported elsewhere.

For **3a** and **9a**, two clearly distinct coalescence processes with different $\Delta G_c^\#$ values were observed, one for each ring. For **3a** the $\Delta G_c^\#$ values differ by 0.9 kcal mol^{-1}. Analogy of the static NMR of **1a**, **3a**, and **9a** suggests that the lower barrier involves a flip of the ring trans to the α-H.

The spectral changes observed for **9a** are shown in Figure 4. Ten methyl signals are observed at 195 K (A), and assignments of pairs of *o*-Me or *m*-Me groups on the same ring are based on the DNMR. Broadening of pairs of signals start at different temperatures (B and C). Four coalescence processes were observed. T_c for the *m*-Me groups at δ 1.98 and 2.15 was determined as 240 K, when the separate signals completely disappeared. The new average signal starts to grow at 245 K (cf. D at 250 K). $\Delta G_c^\#$ = 11.5 ± 0.1 kcal mol^{-1}. Determination of T_c of the other *m*-Me pair at δ 1.962 and 2.146 is difficult due to signals' overlap. It is estimated as 258 ± 5 K from the disappearance of the signals and the appearance of the new signal (cf. E), and $\Delta G_c^\#$ = 12.4 ± 0.25 kcal mol^{-1}. Coalescence of the *o*-Me groups gave $\Delta G_c^\#$ = 11.3 and 12.2 kcal mol^{-1} for the close and the remote pairs of signals, respectively. Consequently, for each ring the $\Delta G_c^\#$'s measured by the two probes were within the combined experimental errors. One average *o*-Me signal is still broad at 313 K well beyond coalescence (G). The spectrum at fast exchange, measured in the higher boiling solvent $Cl_2CDCDCl_2$ at 325 K, shows six sharp singlets (H) one each for the *o*-, *m*-, and *p*-Me group in each ring.

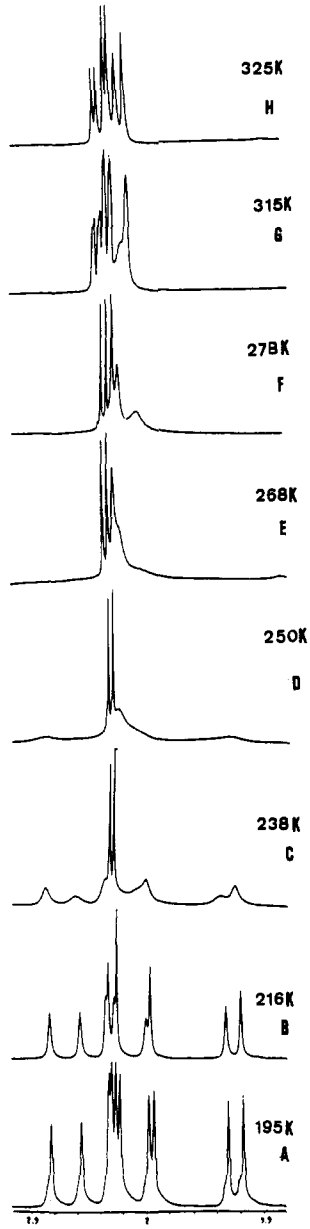

Figure 4. Temperature dependence of the ^{1}H NMR spectrum of **9a**: A, at slow exchange; B and C, signals broadening; D, buildup of average *m*-Me signals after coalescence of a pair of *m*-Me groups at T_c = 240 K (one-ring flip); E, buildup of another average *m*-Me signal after coalescence at T_c = 258 K (a two-ring flip); F, buildup of an average *o*-Me signal after coalescence at T_c = 249 K (a one-ring flip); G, presence of a few sharp and still one broad signal after coalescence of all Me pairs; H, fast-exchange spectrum in $Cl_2CDCDCl_2$.

Enantiomerization was also studied for the isopropyl ether **8** at <222 K; the spectrum is consistent with a frozen propeller conformation (Table V). The isopropyl methyls display an apparent triplet due to overlap of two doublets centered at δ 1.283 and 1.313, which by saturation transfer experiments are involved in a dynamic exchange process. The δ values of 2.607 and 2.614 are assigned as *p*-Me, since they remain sharp on changing the temperature. Irradiation shows that the δ 1.82 and 2.68 methyls participate in one dynamic process and at δ 1.84 and 2.40 in

Table V. ^{1}H NMR Spectra of 2,2-Diaryl-1-R-ethenols and the Enol Ether **8** in 7:3 CD_2Cl_2/CS_2 below and above the Coalescence Temperature

enol	signal	T, K	δ, ppm	T, K	δ, ppm
1a	*o*-Me	175	1.57, 2.42	302	1.43
	o-Me		1.66, 2.31		2.10
	p-Me		2.13, 2.16		2.20, 2.24
	OH		4.85		
	CH		6.25		
	Ar-H		6.57, 6.85		6.86
	Ar-H		6.65, 6.89		
1b	α-Me	225	1.65	266.5	1.68
	o-Me		1.678, 2.33		2.04
	o-Me		1.686, 2.34		
	p-Me		2.17, 2.18		2.19, 2.20
	OH		4.90		4.84
	Ar-H		6.59, 6.86		6.71
	Ar-H		6.65, 6.91		6.80
1d	*t*-Bu	170	1.01	294	1.04
	o-Me		1.80, 1.80		2.12, 2.14
	o-Me		2.38, 2.49		
	p-Me		2.20, 2.22		2.19, 2.20
	OH		4.91		4.85
	Ar-H		6.60, 6.67, 6.83, 6.92		6.69, 6.78
3a	*o*-Me	215	1.84, 2.63	315	2.29
	o-Me		1.88, 2.51		2.34 (br)
	p-Me		2.60		2.68, 2.71
3b	α-Me	186	1.78	293	1.76
	o-Me		1.83, 2.50		2.22, 2.23
	o-Me		1.87, 2.54		
	p-Me		2.64, 2.66		2.66, 2.67
	OH		5.13		4.87
3d	*t*-Bu	167.6	1.10	292	1.09
	o-Me		1.96, 2.46		2.26
	o-Me		1.99, 2.49		2.32
	p-Me		2.61, 2.64		2.63, 2.65
	OH		4.98		4.85
8	*i*-Pr	198	1.28 (d, J = 6.2 Hz)[a]	295	1.28 (d, J = 6.2 Hz)
			1.31 (d, J = 6.2 Hz)[a]		
			4.14 (m)		4.09 (h, J = 6.2 Hz)
	o-Me		1.82, 2.68		2.26 (br)
	o-Me		1.84, 2.40		2.32
	p-Me		2.607, 2.614		2.65
	C-H		6.19		6.24
9a	*o*-Me	185	1.64, 2.27	315[b]	2.09
	o-Me		1.57, 2.41		2.10
	m-Me		1.96, 2.146		2.15
	m-Me		1.98, 2.154		2.18
	p-Me		2.11, 2.13		2.20, 2.31
9b	α-Me	165	1.67	295	1.70
	o-Me		1.63, 2.33		2.03
	o-Me		1.63, 2.35		
	m-Me		2.04, 2.23		2.14, 2.15
	p-Me		2.19 (×2)		2.19, 2.20
9d	*o*-Me	170[b,c]	1.93	293	2.07, 2.11
	m-Me		2.03		2.119, 2.122
	p-Me		2.09		2.17 (×2)

[a] Two overlapping doublets. [b] Assignment at this temperature is unclear due to temperature dependence of δ. [c] Broad signals. Complete decoalescence was not achieved.

Table VI. Comparison of Signal Positions (δ in ppm) in Trimesitylethenol and in its β,β-Bis(dibromomesityl) and β,β-Bis(pentamethylphenyl) Analogs in $C_6D_5NO_2$ at 295 K

assignment	1c	3c	9c[a]
α-*o*-Me	1.93, 2.43	1.89, 2.66	1.94, 2.63
α-*p*-Me	2.14	2.07	1.91
α-Mes-H	6.39, 6.87	6.29, 6.86	6.24, 6.88
β′-*o*-Me	1.84, 2.68	1.98, 2.87	1.80, 2.69
β′-*p*-Me	2.25	2.49	2.11
β-*o*-Me	1.87, 1.98	2.03, 2.13	1.80, 1.89
β-*p*-Me	2.08	2.37	2.14
β-*m*-Me			1.85, 1.94
β′-*m*-Me			1.86, 2.02
OH	5.46	6.11	5.60

[a] Tentative assignments.

another. At 400 MHz, the two isopropyl doublets coalesce at 243 K, giving $\Delta G_c^{\#} = 12.6 \pm 0.1$ kcal mol^{-1} (12.8 ± 0.2 kcal mol^{-1} at 200 MHz). The *o*-Me signals with $\Delta\nu$ = 334.3 and 225 Hz, respectively, coalesce at 304 K and at 282 K, giving $\Delta G_c^{\#}$ values of 13.8 ± 0.1 and 13.0 ± 0.1 kcal mol^{-1} (13.0 ± 0.1 kcal mol^{-1} at 200 MHz). Consequently, the two barriers are distinct. The lower one, observed by coalescence of the *i*-Pr methyl doublets and of the *o*-Me groups of the ring which (by analogy with **3a**) is trans to the α-H, is the threshold barrier with $\Delta G_c^{\#}$ = 12.8 ± 0.2 kcal mol^{-1}. The higher barrier, involving the other ring, is 13.8 ± 0.1 kcal mol^{-1}. The lower barrier is higher than the barrier for the nonbrominated isopropyl ether **12**[4] (Table VII) whereas the higher barrier is higher for **12** than for **8**.

$$Mes_2C{=}CHO\text{-}i\text{-}Pr$$
12

For the α-*tert*-butyl enol **9d**, six relatively sharp methyl singlets, 2.070, 2.108, 2.119, 2.122, 2.168, and 2.175 ppm, are observed at 293 K. At a lower temperature all of them shift to a higher field, the two central *p*-Me signals merge, and several signals broaden. At 170 K there are three broad signals at 1.93, 2.23, and 2.09 ppm. On further temperature lowering, the solvent

Table VII. Rotational Barriers (in kcal mol^{-1}) for the Two Ring Flips of $Ar_2C{=}C(OR')R$

substrate	solvent	$\Delta\nu$, Hz[a]	T_c, K	$\Delta G_c^{\#}$	substrate	solvent	$\Delta G_c^{\#}$
1a	3:7 CS_2/CD_2Cl_2	(i) 263	199	9.0 ± 0.1[b]	**1a**[4]	$(CD_3)_2CO$	10.4 ± 0.05[b]
		(ii) 96.8	193.5	9.1 ± 0.1[b]			14.2
		(iii) 338	302	13.7 ± 0.2			
		(iv) 112.7	286	13.4 ± 0.2			
1b	3:7 CS_2/CD_2Cl_2	(i) 108.4	256	12.0 ± 0.1	**1b**[4b]	$(CD_3)_2CO$	12.6 ± 0.1
		(ii) 100.7	256	12.0 ± 0.2			
3a	3:7 CS_2/CD_2Cl_2	(i) 239.5	264.5	12.1 ± 0.1[b]			
		(ii) 316.5	285.5	13.0 ± 0.1			
3b	3:7 CS_2/CD_2Cl_2	(i) 134	232	10.8 ± 0.1			
		(ii) 128.3	232	10.8 ± 0.1			
3c	$C_6D_5NO_2$	228.8[c]	366	17 ± 0.2[d]	**1c**[5]	$C_6D_5NO_2$	18.4 ± 0.1[d]
3d	3:7 CS_2/CD_2Cl_2	(i) 219.8	180	8.2 ± 0.3	**1d**[4]	$C_6D_5CD_3$	10.4 ± 0.05
		(ii) 226.8					
9a	3:7 CS_2/CD_2Cl_2	(i) 254[e]	249	11.3 ± 0.1[b]			
		(ii) 69[f]	240	11.5 ± 0.1[b]			
		(iii) 334[e]	270	12.2 ± 0.1			
		(iv) 73.5[f]	258 ± 5[g]	12.4 ± 0.25[g]			
9b	3:7 CS_2/CD_2Cl_2	(i) 282, 288[e]	221.4	10.0 ± 0.1			
		(ii) 78[f]	205.5	9.8 ± 0.1			
9c	$C_6D_5NO_2$	(i) 256[c]	359	16.6 ± 0.05			
		(ii) 36[g]	330[h]	17.0 ± 0.3			
		(iii) 62[g]	330[h]	16.7 ± 0.3			
		(iv) 356[e]	350[h]	16.5 ± 0.3			
		(v) 332[e]	350[h]	16.5 ± 0.3			
8	3:7 CS_2/CD_2Cl_2	(i) 334.3	304	13.8 ± 0.1	**12**[4]	$(CD_3)_2CO$	11.1 ± 0.05[b]
		(ii) 225.0	282	13.0 ± 0.1[b]			14.05 ± 0.05
		(iii) 12[i]	243	12.6 ± 0.1			

[a] $\Delta\nu$ between the two coalescing *o*-Me groups at 400 MHz. [b] $\Delta G_c^{\#}$ is for the threshold one-ring flip. [c] *m*-H protons in the α-mesityl ring. [d] For the three-ring flip process. [e] For the *o*-Me groups. [f] For the *m*-Me groups. [g] See text. [h] Tentative value. See text. [i] $\Delta G_c^{\#}$ for coalescence of the isopropyl doublets.

freezes so that $\Delta\nu$ before coalescence and the $\Delta G_c^{\#}$'s could not be measured. We estimate $\Delta G_c^{\#} < 8$ kcal mol^{-1} on the basis of $\Delta\nu$ values for **9a** and **9b**.

The $\Delta G_c^{\#}$ values for **3c** and **9c** were measured from the coalescence of the *m*-H signals of the α-mesityl rings in $C_6D_5NO_2$. At 295 K $\Delta\delta$ of these two protons is 0.57 ppm for **3c** and 0.48 for **1c**, the difference almost exclusively due to the upfield shift of one proton by 0.10 ppm (Table VI). The signals of **3c** coalesce at 366 K, giving $\Delta G_c^{\#} = 17.0 \pm 0.2$ kcal mol^{-1}, 1.4 kcal mol^{-1} lower than for **1c**.[5] A $\Delta G_c^{\#}$ of 16.6 ± 0.05 kcal mol^{-1} for rotation in **9c** was measured *accurately* only from the coalescence of the two *m*-H signals ($\Delta\delta$ = 0.64 ppm at room temperature) of the α-ring at 359 K. At 330 K a small signal starts to form at δ 6.65, and its intensity increases on increasing the temperature. At 432 K it appears at δ 6.75. On cooling to 299 K, the aromatic signal decoalesces, but the new signal remains as a singlet at δ 6.59 with a superimposed singlet at ca. δ 6.58. This is ascribed to oxidation to a benzofuran derivative.[18]

When the temperature is raised, the *p*-Me signals are shifted, new methyl signals are formed, and coalescence processes take place. The *o*-Me and *m*-Me pairs were identified by analogy (Table VI), and from the approximate coalescence temperatures of 350 ± 5 K (*o*-Me) and 330 ± 5 K (*m*-Me) $\Delta G_c^{\#}$ values of 16.5 ± 0.4 and 16.5 ± 0.4 kcal mol^{-1} and 17.0 ± 0.3 and 16.7 ± 0.3 kcal mol^{-1} were calculated.

The barriers for **1a** and **1b** which were previously determined in $(CD_3)_2CO$ and for **1d** in $C_6D_5CD_3$[4] were now investigated in 3:7 CS_2/CD_2Cl_2. The appearance of two different barriers for **1a** and the similar barrier for the two rings of **1b**, with a $\Delta G_c^{\#}$ value between the two barriers for **1a**,[4] is found in both 3:7 CS_2/CD_2Cl_2 and $(CD_3)_2CO$, but the barriers in 3:7 CS_2/CD_2Cl_2 are 0.6–1.3 kcal mol^{-1} lower than in $(CD_3)_2CO$ (Table VII).

Finally, δ(Me) after coalescence is frequently not at the average position of the δ's of the coalescing pair. For example, for **3a** the coalescing *o*-Me signals at δ 1.88/2.51 and 1.84/2.63 ppm at 215 K give at 315 K average signals at δ 2.29 and 2.34, respectively. The downfield shift compared with the calculation is apparently a temperature effect, since, for the noncoalescing *p*-Me signals, δ is 2.60 at 215 K and 2.71, 2.68 at 315 K.

Keto ⇌ Enol Equilibrations. When **3a** and **3b** were kept for 72 h in hexane at 70 °C with a catalytic amount of CF_3COOH, TLC, IR, and ^{1}H NMR analysis showed that no ketonization took place. Since **1d** isomerizes completely to the **1d** ⇌ **2d** equilibrium mixture in 8 h, **3d** was kept for 30, 96, and 192 h under these conditions, giving 4%, 9%, and 25% of **4d**, together with decomposition products, displaying many aliphatic signals. Under the same conditions, **4d** gave <1% of **3d** together with small amounts of decomposition. Even bis(3-bromo-2,4,6-trimethylphenyl)methyl *tert*-butyl ketone does not isomerize after 309 h at 80 ± 1 °C in hexane containing 0.001 mmol of CF_3COOH. Whereas TLC showed the development of a few additional weak new spots, the ^{1}H NMR was identical to that of the ketone.

In contrast, heating 2,2-bis(pentamethylphenyl)-substituted enols and ketones in hexane/CF_3COOH at 80 ± 1 °C leads to equilibration. With **9a**, after 10 h ca. 0.5% of aldehyde **11a** was identified by ^{1}H NMR and its percentage determined by integration of its δ(CH) at δ 9.89 ppm. Equilibration of **9b** was achieved after 20 h, when ketone **11b** consists of ca. 22% of the equilibrium mixture. **11b** which was isolated from this experiment gave after 8 h in hexane/TFA the same **9b**/**11b** ratio.

Enol **9d** isomerized relatively rapidly to an ca. 98:2 **11c**/**9d** mixture, and **11c** which was isolated from the mixture gave the same equilibrium ratio.

The equilibration data are given in Table VIII. As with enols **1** ⇌ ketones **2**, the equilibrium constants K_{enol} decrease strongly with the increase in the bulk of R, by ca. 8800-fold from **9a** to **9d**.

Discussion

We first looked for a buttressing effect by comparing dimesitylethenols **1** and their tetrabromo derivatives **3**.[1b] However, the slow or unobservable ketonization of enols **3** and the conclusion that the $\Delta G_c^{\#}$ difference between systems **1** and **3** is due to electron withdrawal by the bromines led to study of some β,β-bis(pentamethylphenyl)ethenols **9**. We searched for buttressing in four different phenomena: (1) the ease of synthesis of the enols, (2) the K_{enol} values, (3) the ground-state crystallographic structures, and (4) the Ar—C=C rotational barriers. We found that differences due to buttressing by four *m*-Br or four *m*-Me sub-

(18) The colors observed during synthesis are attributed to the oxidation of these electron-rich enols.

Table VIII. K_{enol} Values for Enols 9 ⇌ Ketones 11 in Hexane at 80 ± 1 °C

substrate	reaction time, h	% enol	K_{enol}	K_{enol}[a] (average)	K_{enol}[b] (average)
9a	10	99.45	182		
	15	99.45	182	185	185
	30	99.47	189		
9b	4.5	81.9 ± 0.6	4.5		
	12	74.1 ± 0.9	2.9		
	15	76.7	3.3		
	27	78.6 ± 1.3	3.7		
	60	78.6	3.7	3.6	3.6
11b	8	78.1	3.6	3.6	
9d	5	3.7	0.038		
	10	1.0	0.010		
	26	2.3	0.023	0.021	
	4.5	1.5	0.016		
	20	1.5	0.016		0.021
11c	5	2.2	0.022		
	10	1.7	0.017		
	26	2.8	0.029		
	4.5	2.6	0.027	0.021	
	10	1.1	0.011		

[a] Average of the last points starting from a single species. [b] Average of K_{enol} starting from both sides.

stituents are not large although they are mostly systematic.

(1) Effect of Meta Substituents on the Synthesis of the Enols. Except for differences due to the lower solubility of tetrabromodimesitylketene (**5**) compared with dimesitylketene, formation of enols **3a–c** qualitatively resembles that of their analogs **1a–c**. The difficulty in preparing **3d** by eq 2 is due to a Li/Br exchange which destroys both reagents. The ready formation of the enols **9a–d** from the lithium reagents and ketene **10** corroborates this conclusion.[18] Consequently, we see no synthetic manifestation of buttressing by the *m*-Br or *m*-Me groups.

(2) Differences in Keto ⇌ Enol Equilibrations. Whereas TFA-catalyzed equilibration of enols **1a–d** in hexane proceeds from both sides, it was not achieved even after much longer reaction times starting from enols **3**. The reason is not thermodynamic, since under the same conditions **1a** and **1d** consist of ca. 95% and <1% of the equilibrium mixture so that, if the four bromines either increase or decrease K_{enol} (eq 6), one of the enols **3a** and **3d** should

$$\text{carbonyl compound (2, 4, or 11)} \overset{K_{enol}}{\rightleftharpoons} \text{enol (1, 3, or 5)} \qquad (6)$$

be in excess and the other in deficiency at equilibrium. Analogy with the increase of K_{enol} by electron-withdrawing substituents in 2-arylpropen-1-ols[19] predicts K_{enol} values of >20 and >0.006 for **3a** and **3d**, respectively.

A slow approach to equilibrium was observed starting from **3d**. A priori, the slow or nonobservable equilibrations may be due to buttressing, but an electronic effect is of major importance. Electron withdrawal by four bromines reduces appreciably the nucleophilicity of the double bond, whose protonation is rate determining in the isomerization. Since protonation is slow even for enols **1**, a high kinetic barrier for the isomerization is apparent. The slow competing reaction which consumes the enol could be partially due to the efficiency of TFA, which may serve as a single-electron oxidant.[20]

Even two bromines reduce completely the isomerization rate from the ketone side, since 2,2-bis(3-bromo-2,4,6-trimethylphenyl)methyl *tert*-butyl ketone does not isomerize after 309 h.

The operation of an electronic effect is corroborated by the equilibration of the *m*-methyl-substituted enols **9a–c** in <30 h (Table VIII) in hexane at 80 ± 1 °C, which seems qualitatively faster than equilibration of enols **1** under similar conditions. The three enols investigated cover almost the entire range of equilibrium mixtures that are experimentally observable by NMR, from 99.5% enol for **9a** ⇌ **11a** to 1–2% enol for **9d** ⇌ **11c**.

In both series **1**[4] and **9** the smaller the aliphatic α-R, the higher the K_{enol}. Decreased β-Ar—C=C conjugation and an increased C=C torsional angle in the bulkier systems and different R—C=C hyperconjugation in **9** than in **11** are the main reasons for this order. Also, K_{enol} values for **9** are consistently higher: $K_{enol}(\mathbf{9a})/K_{enol}(\mathbf{1a}) \approx 9$, $K_{enol}(\mathbf{9b})/K_{enol}(\mathbf{2b}) = 5.6$, and $K_{enol}(\mathbf{9d})/K_{enol}(\mathbf{1d}) \approx 3.6$. More quantitative conclusions from these ratios are unwarranted.

The combined electronic effect of the four *m*-Me groups ($\sigma_{m\text{-Me}} = -0.07$) on K_{enol} is negligible. For example, K_{enol}(ArC(Me)=CHOH) = 0.096 and 0.097 in DMSO when Ar = Ph and *m*-MeC_6H_4, respectively.[19] The torsional angle differences between **1a** and **9a** and **1d** and **9d** are small and in opposite directions (Table IV), indicating similar extents of Ar—C=C conjugation in **1** and **9**.[21] Consequently, the $K_{enol}(\mathbf{9})/K_{enol}(\mathbf{1})$ ratios reflect a nearly pure buttressing effect.

The increase of K_{enol} values by buttressing should be due to increased constraint in movements of the *o*-Me groups in both the ketones and the enols. The steric factor which increases the stability of the β,β-diaryl- over simple β,β-dialkyl-substituted enols operates here as well. Intuitively, the main factor in increasing the relative stability of the enols is a steric interaction at C_β of the sp^2-hybridized enols that is lower than that in the sp^3-hybridized ketones. However, since the bond angles of both species differ from the ideal sp^2- and sp^3-angles and the overall effect is small, other factors may also influence the increase in the K_{enol} values of **9** over those of **1**.

(3) Crystallographic Structure. The main deduction from Tables I–IV is that buttressing by the *m*-Br or the *m*-Me groups mostly affects only slightly the solid-state structures of the 2,2-dimesitylethenols. The effect, if any, should be more pronounced for the α-*tert*-butyl derivative. However, the Δ^{31} and Δ^{91} values of Table IV which compare the tetra-*m*-H to the tetra-*m*-Br and tetra-*m*-Me derivatives are remarkably close to zero when R = *t*-Bu for all bond angles except one. Moreover, the torsional angles $\Delta\phi_2$ and especially $\Delta\phi_1$ are negative when R = *t*-Bu. Considering that ϕ_2 changes from 56.7° for **1a** to 63.7° for **1d**, the buttressing effect is very small, or in the opposite direction, for the more crowded enols.

Of the 32 measured bond angles for all enols, the Δ's are >2° only in five cases. However, differences do occur in the Ar—C=C torsional angles of the formally less crowded enols. The $\Delta\phi_1$ and $\Delta\phi_2$ values are positive, the larger being $\Delta\phi_2$ for R = H and $\Delta\phi_1$ for R = Mes. The bond lengths are also practically unaffected by the presence of the meta substituents.

We note that MM calculations on tetramesitylethylene and its octabromo derivative give very similar torsional and bond angles in both species.[22]

Changes due to the *m*-bromo substituents of **3** occur in angles around the meta positions of the rings. The inter-ring $C_oC_mC_p$ angles increase from an average of 123.8° for **3a** to an average of 125.3° for **3d**, with a compensation by the $C_mC_pC_m$ angles which are mostly 114–116°. The inter-ring bond angle near an electron-withdrawing substituent usually opens. While a value for bromine was not found, the angle should increase by 1.5–2°, judging from data on chloro derivatives.[23] The internal bond angles around the carbon bonded to Br are 123.9–125.9° for 1,3,5-trineopentyl-2,4,6-tribromobenzene.[24a] However, they are 120.0–121.2° in 1,4-dibromo-2,5-diethyl-3,6-dimethylbenzene[24b] and in 1,3-dibromo-2,5-diethyl-4,6-dimethylbenzene.[24b] The bond angles involving the *o*-Me groups show little evidence of but-

(19) Ahlbrecht, H.; Funk, W.; Reiner, M. T. *Tetrahedron* **1976**, *32*, 479.
(20) Eberson, L.; Radner, F. *Acta Chem. Scand.* **1991**, *45*, 1093.
(21) This argument involves the assumption that the unknown geometries of the carbonyl isomers **2** and **11** are also very similar.
(22) Gur, E.; Kaida, Y.; Okamoto, Y.; Biali, S. E.; Rappoport, Z. *J. Org. Chem.* **1992**, *57*, 3689.
(23) (a) Krygowski, T. M. *Prog. Phys. Org. Chem.* **1990**, *17*, 239. (b) Domenicano, A.; Mazzeo, P.; Vaciago, A. *Tetrahedron Lett.* **1976**, 1029. Domenicano, A.; Murray-Rust, P. *Tetrahedron Lett.* **1979**, 2283, and other papers by Domenicano's group on aromatic substituent effects on distortion of the ring angle.
(24) (a) Aurivillius, B.; Carter, R. E. *J. Chem. Soc., Perkin Trans. 2* **1978**, 1033. (b) Wood, R. A.; Welberry, T. R.; Puza, M. *Acta Crystallogr. C: Cryst. Struct. Commun.* **1984**, *40*, 1255.

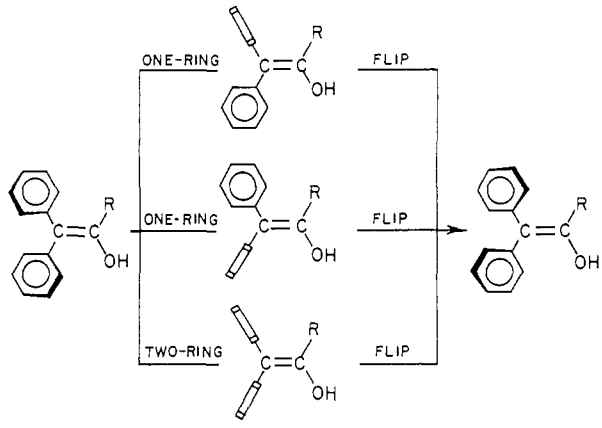

Figure 5. "Ideal" transition states for one- and two-ring-flip processes in vinyl propellers. ▭ indicates a ring which is perpendicular to the C=C bond. Aromatic substituents are not shown for simplicity.

tressing. The $C_mC_oC_{Me}$ angles for **3** are ca. 120° while the $C_{ipso}C_oC_{Me}$ angles are around 122° and for **9** around 121°, whereas the $C_mC_pC_{Me}$ angles for **3** are ca. 122° and ca. 120° for **9**.

Three possible hydrogen bond arrangements, i.e., (a) intramolecular π(Ar)—OH with a syn C=C—O—H conformation, (b) intermolecular enol–enol, and (c) enol·solvating hydrogen-bond-accepting solvent with an anti C=C—O—H conformation, were found: (a) for **3d** and **9d**, (b) for **9a**, and (c) for **3b**·Et_2O. Precedents for (a), with e.g. **1d**, (b) **1a**, and (c) e.g. **1b**·EtOH, were previously recorded and discussed.[3a] Due to the close analogy with our compounds, the discussion will not be repeated here.

(4) Rotational Barriers. We previously concluded[4,5] that the rotation of the two or the three rings around the Ar—C=C bonds in enols **1** is correlated. In the "ideal" transition state a ring can be perpendicular to the C=C bond (a flip process) or in its plane (a nonflip process). Each process leads to helicity reversal, i.e., to propeller enantiomerization (Figure 5). By analogy, and using similar mechanistic criteria, we assume that the rotations in systems **3** and **9** are also correlated.

The threshold (lower energy) rotational mechanisms observed for enols **1**, i.e., a one-ring flip when R = H, a two-ring flip when R = Me or *t*-Bu, and a three-ring flip when R = Mes,[5] were also observed for **3** and **9**. However, there are consistent quantitative differences between the three systems.

The threshold rotational process for **1a** in $(CD_3)_2CO$ is a one-ring flip, where the ring cis to the hydrogen passes through the C=C plane. The *o*-Me groups of the other ring coalesce with a barrier higher by 3.8 kcal mol^{-1} which was ascribed to a two-ring flip[4] (Table VII). Two easily distinguishable barriers were also observed now for **3a** and **9a** in 3:7 CS_2/CD_2Cl_2, but with a gap of only 0.9 kcal mol^{-1} in both systems (Table VII). Both barriers for **1a** were found now to be lower in CS_2/CD_2Cl_2 than in $(CD_3)_2CO$: the one-ring flip by 1.3 kcal mol^{-1} and the two-ring flip by 0.7 kcal mol^{-1}, i.e., the barriers differ by 4.4 kcal mol^{-1}.

The much lower difference in $\Delta G_c^{\#}$ between the two barriers for **3a** and **9a** compared with **1a** calls for corroboration of the conclusion that the one-ring flip is the threshold mechanism. The two isopropyl methyl groups of the ether **8** are diastereotopic due to the propeller part of the molecule, and propeller enantiomerization was accompanied by coalescence of the two isopropyl doublets. Since the barrier measured by this enantiomerization probe resembles the one-ring-flip barrier measured by the coalescence of the *o*-Me groups and is lower than that for the two-ring flip, the one-ring flip is the threshold mechanism. The barriers for **8** are 0.7–0.8 kcal mol^{-1} higher than those for **3a** (Table VII). This difference is similar to that between the lower barrier for **1a** and that for its isopropyl ether (**12**), whereas the higher barrier is almost the same for both compounds in $(CD_3)_2CO$.[4]

In 3:7 CS_2/CD_2Cl_2, the barriers for the one-ring flip in **3a** and **9a** are significantly higher, by 3.0 and by 2.3 kcal mol^{-1}, than that for **1a**. Such a "positive buttressing effect"[11a] is well documented.[11,12] In contrast, all the two-ring-flip barriers are higher for **1**, exemplifying the less common "negative buttressing effect".[11a] We believe that the "positive" effect for the one-ring flip is the most straightforward manifestation of buttressing. The passage of the di-*m*-X-substituted ring (X = Me or Br) cis to the hydrogen through the C=C plane in the transition state is energetically more costly than when X = H due to the *o*-Me/H steric interaction. Indeed, the one-ring flip is the threshold mechanism when R = H even when the β-aryl is substituted by the two bulkier *o*-isopropyl groups.[8] This vicinal interaction is larger when R is bulkier than hydrogen, and the preferred threshold mechanism is a two-ring flip in which this interaction is completely avoided.

With **3b**, **3d**, and **9b**, the coalescence of the *o*-Me groups gives essentially the same barrier for the two rings in each system (Table VII). This is consistent with a two-ring-flip process, and these barriers and those for **3a** and **9a** show a negative buttressing effect. They are lower by 0.8 kcal mol^{-1} when R = H or Me for enols **9** than for enols **3**, and the latter are 0.6–2.2 kcal mol^{-1} lower than those for enols **1**. Likewise, the three-ring-flip barriers for **3c** and **9c** are lower by 1.4 and 1.8 kcal mol^{-1} than those for **1c** (Table VII).

Negative buttressing effects are ascribed to higher destabilization of the ground state than of the transition state.[11a] The lower barriers for **3** and **9** could be explained similarly if the torsional Ar—C=C angles would be higher than those for the analogous **1**. We calculated the contribution of this effect by assuming a $\cos^2$ dependence on the extent of conjugation of the aryl and C=C π-systems. For the α-H enols where the torsional angles, except one, are higher for **3** and **9** by several degrees, the $\sum(\cos^2\phi_1 + \cos^2\phi_2)$ values are 0.71 (**1a**), 0.58 (**3a**), and 0.57 (**9a**). For a Ph_2C=C conjugation energy of 9.0 kcal mol^{-1} at full planarity,[25] such values amount to 3.2 (**1a**), 2.6 (**3a**), 2.5 (**9a**), 2.75 (**1b**), 2.1 (**3b**), 4.65 (**1c**), and 3.7 (**3c**) kcal mol^{-1} conjugation energy. Consequently, the ground-state energy increases by 0.6–0.95 kcal mol^{-1} before correcting for the electronic effect. If similar conformations exist in solution, an appreciable part of the lower $\Delta G_c^{\#}$ for **3a**, **3b**, and **9a** for the two-ring flip is due to this effect. However, for **3d** and **9d** where the torsional angles are lower than those in **1d**, the corresponding Ar—C=C stabilizations of 1.6 (**1d**), 2.0 (**3d**), and 2.0 (**9d**) kcal mol^{-1} should *increase* the barrier by 0.4 kcal mol^{-1}.

The uncertainty in such calculations is estimated as ≥0.4 kcal mol^{-1} from the two values based on the different Ar—C=C torsional angles in the two structurally independent molecules in the unit cell of **9a** (Table III): 2.7 (**9a**, A) and 2.3 (**9a**, B) kcal mol^{-1}.

However, conjugation is not the predominant factor responsible for the barrier. Comparing the values calculated above with the barriers in Table VII shows that the complete loss of conjugation amounts to only 19–25% of the $\Delta G_c^{\#}$ values.

The *calculated* Ar—C=C conjugation contribution to the $\Delta G_c^{\#}$'s difference between the one- and two-ring flips of the same system favors the former by 4.5 kcal mol^{-1} for systems **1** and **9** and by 4.1 kcal mol^{-1} for systems **3** (see below), provided that the nonflipping ring is not distorted at the ideal transition state with $\phi_2 = 0$. The *experimental* preferences for the one-ring flip in **1a**, **3a**, and **9a** are 4.6, 0.9, and 0.9 kcal mol^{-1}. Consequently, for **1a**, steric interaction of the nonflipping cis-Ar/vinylic-H contributes very little to the transition-state energy. Hence, the reduction of the differences for **3a** and **9a** by 3.6 and 3.2 kcal mol^{-1} is due to a combination of the one-ring-flip transition-state destabilization by the *cis*-Ar/vinylic-H interaction and a corresponding stabilization/destabilization of the two-ring-flip transition state by buttressing. For **3a** and **9a** the latter values are the negative buttressing effects of 0.6 and 1.3 kcal mol^{-1}, respectively. Consequently, the "corrected" buttressing effects on the Ar/H interaction in the one-ring flip are 3.0 and 1.9 kcal mol^{-1} for the di-*m*-Br- and the di-*m*-Me-substituted rings.

Within each series, the $\Delta G_c^{\#}$ decreases with the increased bulk of R, as for enols **1**,[4] partially due to the higher ground-state torsional Ar—C=C angles (Table III) and hence to a larger extent

(25) Hine, J.; Skoglund, M. J. *J. Org. Chem.* **1982**, *47*, 4766.

of deconjugation for the bulkier R. Since deconjugation is complete in the transition state for the rotation of all enols, the barrier is lower for bulkier R's.

The differences in the Ar—C=C conjugation term between the α-H and the α-*t*-Bu enols are 1.6, 0.6, and 0.5 kcal mol^{-1} for systems **1**, **3**, and **9**. Since the experimental differences for the two-ring flips are 3.6 (in $C_6D_5CD_3$ vs 3:7 CS_2/CD_2Cl_2) for **1**, 4.8 for **3**, and >4.3 kcal mol^{-1} for **9**, this ground-state effect is insufficient to account completely for the barrier. Hence, electronic effects of the four substituents should be considered. The Ar—C=C conjugative stabilization energy decreases by electron-withdrawing substituents[25] at full planarity from 4.53 kcal mol^{-1} for Ar=Ph to 4.50 and 4.38 kcal mol^{-1} for *p*-ClC_6H_4 and *m*-FC_6H_4, respectively. A value for *m*-BrC_6H_4 is unavailable, but from a Hammett plot we estimate it to be 4.33 kcal mol^{-1}, i.e., 0.8 kcal mol^{-1} for four *m*-Br at full conjugation. From the values calculated above for Ar = Ph, we obtain the "electronically corrected" Ar—C=C stabilizations of 2.1 (**3a**), 1.7 (**3b**), 3.0 (**3c**), and 1.6 (**3d**) kcal mol^{-1}. The derived calculated reductions of the barriers by 1.1 (**1a** ⇌ **3a**), 1.0 (**1b** ⇌ **3b**), 1.7 (**1c** ⇌ **3c**), and 0 (**1d** ⇌ **3d**) kcal mol^{-1} account for all the observed values except that for **3d**.

A *m*-Me group has a minor electronic effect compared with hydrogen. Both extrapolation of Hine's data[25] and the almost identical K_{enol} values for ArC(Me)=CHOH, Ar = Ph or *m*-MeC_6H_4,[19] are consistent with a negligible electronic effect on the barrier. However, the combined electronic/conjugation effect contributes 0.4–0.5 kcal mol^{-1} more to the lower barriers for enols **9** than for **3**. This accounts for all of the difference for **3c** ⇌ **9c** and for an appreciable part of it for the other enols.

The most likely main contributor to the barrier is the repulsive interaction between *o*-Me groups on neighboring rings in the transition state. Similar interaction between meta substituents is less important. If buttressing reduces the distance between these *o*-Me groups even slightly, the barrier will decrease, but we have no probe to this question.

Solvent effects on rotational barriers in non-hydrogen bond accepting solvents are usually small.[26] However, differences of up to 1.7 kcal mol^{-1} were found when an intramolecular (π-Ar)–OH hydrogen bonding which stabilizes the ground state in a non-hydrogen bond accepting solvent is replaced by an OH–solvent interaction in an hydrogen bond accepting solvent.[27] For **1a** and **1b**, the OH···π(*cis*-Ar) hydrogen bond in 3:7 CS_2/CD_2Cl_2 is mainly replaced by a bond to the solvent in $(CD_3)_2CO$. The lower two-ring-flip barrier in CS_2/CD_2Cl_2 can therefore reflect an increase in this OH–π(Ar) interaction in the transition state when the aryl group and the OH are orthogonal.

Conclusion. The buttressing by four *m*-Br or four *m*-Me groups was investigated by more probes and in more compounds than in earlier cases.[11,12,26] The effect is reflected by (i) a moderate increase in the K_{enol} values, (ii) an increase in the barrier of the one-ring flip where a buttressed ring interacts sterically with the vinylic hydrogen in the transition state, and (iii) a "negative buttressing effect" for the two-ring flip. Buttressing mostly affects the solid-state geometry only slightly, but not in the same direction for all compounds.

Experimental Section

General Methods. Melting points were determined with a Thomas–Hoover apparatus and are uncorrected. UV spectra were taken with a Uvikon-930 spectrometer and IR spectra with a Perkin-Elmer Model 157G and FTIR 1600 spectrometers. EI mass spectra were recorded with a MAT-311 instrument at 70 eV, CI spectra with a Finnigan 4021 spectrometer, and high-resolution spectra with a MAT-711 instrument. ^{1}H NMR spectra were recorded on Bruker WP 200 SV and AMX 400 pulsed FT spectrometers operating at 200.133 and 400.266 MHz, and ^{13}C NMR spectra were recorded on the same spectrometers operating at 50.32 and 100.62 MHz, respectively, with TMS as a reference.

Solvents and Materials. THF was stored over benzophenone ketyl, and ether was kept over $LiAlH_4$. They were distilled before use under argon. CCl_4 was dried over 4A molecular sieves. Other solvents were commercial samples and were used without further purification. Commercial solutions (Aldrich) of MeLi (1.4 M in ether), *t*-BuLi (1.6 M in hexane or 1.7 M in pentane), and MesMgBr (1 M in THF) were handled in an inert atmosphere.

Tetrabromodimesitylacetic acid and tetrabromodimesitylketene were prepared according to Biali et al.,[13] and bis(pentamethylphenyl)acetic acid and the corresponding ketene were prepared according to Hegarty et al.[15]

2,2-Bis(3,5-dibromomesityl)ethenol (3a). To a brown-yellow solution of bis(3,5-dibromomesityl)ketene (400 mg, 0.68 mmol) in dry THF (10 mL) was slowly added $LiAlH_4$ (40 mg, 1.05 mmol). The solution turned first light yellow and then light green after 30 min. After the solution was stirred for 1 h (the solution turned light pink), water (3 drops) was added to destroy the unreacted $LiAlH_4$. Anhydrous $MgSO_4$ (50 mg) was added, and the inorganic salts were filtered off. Evaporation of the filtrate gave 2,2-bis(3,5-dibromomesityl)ethenol as a light pink solid (196 mg). 3% HCl (10 mL) was then added to the precipitate, which was extracted with ether (5 × 4 mL). Evaporation of the ether gave additional enol (199 mg, total yield 79%). The crude pink product was chromatographed on a dry silica column using 85:15 petroleum ether/ether eluent. Crystallization (MeOH) gave 240 mg (60%) of pure 2,2-bis(3,5-dibromomesityl)ethenol (**3a**), mp 206 °C. UV (hexane) λ_{max} (ε): 237 sh (56 000), 259 sh (15 000) nm. IR (Nujol) ν_{max}: 3500 (OH, w), 1610 (C=C, m) cm^{-1}. ^{1}H NMR ($CDCl_3$, room temperature) δ: 2.29 (12 H, s, *o*-Me), 2.69, 2.71 (2 × 3 H, 2 s, *p*-Me), 4.78 (1 H, d, *J* = 12.5 Hz, OH), 6.39 (1 H, d, *J* = 12.5 Hz, CH). Mass spectrum *m*/*z* (relative abundance, assignment): 600, 598, 596, 594, 592 (17, 67, 100, 68, 17, M), 519, 517, 515, 513 (21, 60, 62, 22, M – Br), 438, 436, 434 (34, 54, 25, M – 2Br), 358 (22), 237 (24), 217 (42), 202 (44), 129 (46). Anal. Calcd for $C_{20}H_{20}Br_4O$: C, 40.36; H, 3.19. Found: C, 40.07; H, 3.49.

1,1-Bis(3,5-dibromomesityl)-1-propen-2-ol (3b). To a stirred brown solution of bis(3,5-dibromomesityl)ketene (297 mg, 0.3 mmol) in dry THF (20 mL) at −18 °C under Ar was slowly injected during 10 min a solution of MeLi in ether (1.4 M, 0.45 mL, 0.6 mmol). The yellow mixture was stirred for an additional 3 h and then poured into a 5% solution of aqueous NH_4Cl (20 mL) and ice (55 mL). The mixture turned pink, and a solid precipitated. The mixture was extracted with ether (3 × 15 mL), the phases were separated, the organic phase was washed with water (15 mL) and dried ($MgSO_4$), and the solvent was evaporated. The remainder (290 mg, 95%) was chromatographed on silica using 85:15 petroleum ether (40–60 °C)/ether as eluent, giving white crystals of the crude ethenol (128 mg, 40%). Crystallization (MeOH) gave pure 1,1-bis(3,5-dibromomesityl)-1-propen-2-ol (**3b**), (100 mg, 32%), mp 202 °C. UV (hexane) λ_{max} (ε): 227 sh (48 000), ca. 261 sh (12 000) nm. IR (Nujol) ν_{max}: 3500 (OH, w), 1620 (C=C, m) cm^{-1}. ^{1}H NMR ($CDCl_3$, room temperature) δ: 1.78 (3 H, s, Me), 2.25 (12 H, s, *o*-Me), 2.69, 2.70 (2 × 3 H, 2 s, *p*-Me), 4.86 (1 H, s, OH). Mass spectrum (180 °C, 70 eV) *m*/*z* (relative abundance, assignment): 614, 612, 610, 608, 606 (2, 8, 13, 9, 2, M), 452, 450, 448 (9, 17, 8, M – 2Br), 333, 331, 329 (1.7, 3, 1.6, M – H_2 – Br_2Mes), 43 (B, MeCO). Anal. Calcd for $C_{21}H_{22}Br_4O$: C, 41.37; H, 3.64. Found: C, 41.54; H, 3.63.

2,2-Bis(3,5-dibromomesityl)vinyl Isopropyl Ether (8). To a solution of enol **3a** (89.4 mg, 0.15 mmol) and Bu_4NBr (12.1 mg, 0.38 mmol) in 2-bromopropane (1.9 mL) was added a solution of 50% aqueous NaOH (2 mL), and the mixture was stirred overnight at room temperature. Ether (10 mL) was then added, the phases were separated, and the organic phase was washed with water (2 × 10 mL), dried ($MgSO_4$) and evaporated, giving a colorless solid, mp 169–175 °C. Crystallization from 1:1 $EtOH/CH_2Cl_2$ gave colorless crystals (58 mg, 65%) of 2,2-bis(3,5-dibromomesityl)vinyl isopropyl ether (**8**), mp 189 °C. UV (hexane) λ_{max} (ε): 207 nm (66 000), 262 sh (15 000), 228 sh (34 000) nm. IR (Nujol) ν_{max}: 1620 (C=C, m) cm^{-1}. ^{1}H NMR ($CDCl_3$, room temperature) δ: 1.28 (6 H, d, *J* = 6.5 Hz, *i*-Pr-Me), 2.23, 2.36 (12 H, 2 br s, *o*-Me near coalescence), 2.68 (6 H, s, *p*-Me), 4.1 (1 H, m, C*H*Me$_2$), 6.24 (1 H, s, =CH). Mass spectrum (130 °C, 70 eV) *m*/*z* (relative abundance, assignment): 642, 640, 638, 636, 634 (6, 23, 33, 22, 6, M), 600, 598, 596, 594, 592 (8, 30, 47, 33, 9, MH – *i*-Pr (**3a**)), 519, 517, 515, 513 (22, 70, 78, 31, M – Br – *i*-Pr), 438, 436, 434 (39, 54, 23, M – 2Br – *i*-Pr), 358, 356 (32, 33, MH – 3Br – *i*-Pr), 239 (25), 237 (24), 217 (33), 216 (24), 215 (26), 203 (22), 202 (25), 43 (B, MeCO). Anal. Calcd for $C_{23}H_{26}Br_4O$: C, 43.29; H, 4.16; Br, 50.9. Found: C, 43.17; H, 4.09; Br, 48.75.

2,2-Bis(3,5-dibromomesityl)-1-mesitylethenol (3c). To a stirred solution of mesityl MgBr (Aldrich, 0.5 mL of 1 M solution in THF, 0.5 mmol) in dry THF (95 mL) was slowly injected bis(3,5-dibromo-

(26) Oki, M. *Applications of Dynamic NMR Spectroscopy to Organic Chemistry*; VCH Publishers: New York, 1990.

(27) (a) Oki, M.; Iwamura, H.; Nishida, T. *Bull. Chem. Soc. Jpn.* **1968**, *41*, 656. (b) Oki, M.; Akashi, K.; Yamamoto, G.; Iwamura, H. *Bull. Chem. Soc. Jpn.* **1971**, *44*, 1683.

(28) (a) Biali, S. E.; Rappoport, Z. *J. Am. Chem. Soc.* **1984**, *106*, 5641. (b) Nadler, E. B.; Rappoport, Z. *J. Am. Chem. Soc.* **1989**, *111*, 213.

mesityl)ketene (200 mg, 0.34 mmol) in THF (10 mL) during 20 min. After reflux for 4 h, the red solution was poured into a 5% NH_4Cl solution (10 mL + ice), washed with water (2 × 10 mL), extracted with ether (3 × 10 mL), dried ($MgSO_4$), and evaporated. Chromatography of the rosy oily precipitate (180 mg) on dry silica (Woelm TSC) using 95:5 petroleum ether/ether eluent gave 2,2-bis(3,5-dibromomesityl)-1-mesitylethenol (**3c**) (78 mg, 44%). Crystallization (EtOH) gave pure **3c**, mp 164 °C. IR (Nujol) ν_{max}: 3500 (OH, w), 1620 (C=C, s) cm^{-1}. ^1H NMR ($CDCl_3$, room temperature) δ: 1.83 (3 H, s, Me), 2.01 (3 H, s, Me), 2.23 (9 H, s, Me), 2.44 (3 H, s, Me), 2.61 (3 H, s, Me), 2.71, 2.72 (6 H, 2 s, 2 Me), 5.02 (1 H, s, OH), 6.63, 6.91 (2 H, 2 s, Mes-H). Mass spectrum (180 °C, 70 eV) *m/z* (relative abundance, assignment): 718, 716, 714, 712, 710 (9, 32, 48, 32, 8, M), 638, 636, 634, 632 (2, 6, 7, 3, MH - Br), 556, 554, 552 (3, 6, 3, M - 2Br), 147 (B, MesCO), 119 (45, Mes), 91 (15, C_7H_7), 43 (7, MeCO). Anal. Calcd for $C_{29}H_{30}Br_4O$: C, 48.77; H, 4.24. Found: C, 48.48; H, 4.23.

1-*tert*-Butyl-2,2-dimesitylvinyl Acetate (6). To 2,2-dimesityl-1-*tert*-butylethenol (0.68 g, 2 mmol) in dry pyridine (8 mL) was added acetic anhydride (3.0 mL, 30 mmol). The mixture was stirred under reflux for 8 h. Its color was light orange, orange-brown, and brown after 0.25, 4, and 7 h. The mixture was poured into ice–water (100 mL), $CHCl_3$ (50 mL) was added, and after the filtration the organic phase was separated. The aqueous phase was extrated three times with $CHCl_3$ (3 × 50 mL), and the combined organic phase was dried ($MgSO_4$) and evaporated. Chromatography on a dry silica column (Woelm TSC) using 3:1 petroleum ether/CH_2Cl_2 eluent gave a solid (403 mg, 58%). Crystallization (EtOH) gave pure 2,2-dimesityl-1-*tert*-butylvinyl acetate (6), mp 127 °C. IR (Nujol) ν_{max}: 1740 (C=O), 1600 (C=C) cm^{-1}. ^1H NMR ($CDCl_3$, room temperature) δ: 1.03 (9 H, s, *t*-Bu), 1.57, 1.64 (3 H, 2 s, 2 OAc conformers), 1.88 (6 H, br s, *o*-Me), 2.18, 2.22 (6 H, 2 s, *p*-Me), 2.44 (3 H, br s, *o*-Me), 2.73 (3 H, br s, *o*-Me) (broad due to coalescence), 6.73, 6.82 (4 H, 2 br m, Mes-H). Mass spectrum (70 °C, 70 eV) *m/z* (relative abundance, assignment): 378 (18, M), 336 (85, M - CH_2CO), 251 (18, Mes_2CH), 235 (10, Mes_2C - Me), 221 (12, Mes_2CH - 2Me), 205 (B, Mes_2C - 3Me). Mass spectrum (60 °C, 70 eV) *m/z* (relative abundance, assignment): 338 (17, M), 336 (B, M - CH_2CO), 251 (17, Mes_2CH), 235 (13, Mes_2C - Me), 220 (Mes_2CH - 2Me), 57 (72, *t*-Bu). Anal. Calcd for $C_{26}H_{34}O_2$: C, 82.49; H, 9.05. Found: C, 82.21; H, 9.00.

The chromatography also gave the known[6,29] *tert*-butyl dimesitylmethyl ketone (**2d**), mp 97 °C (40 mg, 5.7%). IR (Nujol) ν_{max}: 1730 (C=O), 1620 (C=C) cm^{-1}. ^1H NMR ($CDCl_3$, room temperature) δ: 1.19 (9 H, s, *t*-Bu), 2.11 (12 H, s, 4 *o*-Me), 2.22 (6 H, s, 2 *p*-Me), 5.62 (1 H, s, CH), 6.72 (4 H, s, Mes-H).

Bromination of 1-*tert*-Butyl-2,2-dimesitylvinyl Acetate (6). **(a) Incomplete Bromination.** To a stirred mixture of 6 (0.3 g, 0.8 mmol) and granular (60 mesh) iron (15 mg, 0.2 mmol) in CCl_4 (10 mL) was added bromine (0.17 mL, 3.2 mmol) in CCl_4 (4.5 mL) dropwise in the dark at room temperature during 1 h. The solution turned light brown, and HBr was evolved. After the solution was stirred for an additional h, 5% aqueous $Na_2S_2O_3$ solution (2 × 20 mL) was added until the discharge of the bromine color. Water (30 mL) and CCl_4 (30 mL) were added, the phases were separated, the organic phase was dried ($MgSO_4$), and the solvent was evaporated, giving a yellow oil (380 mg). The ^1H NMR ($CDCl_3$) of the crude solution showed aromatic protons at δ 6.74, 6.78, and 6.91. Chromatography on silica using 4:1 petroleum ether/CH_2Cl_2 eluent gave several fractions containing mixtures of polybrominated acetates. Three of them showed the following properties:

I. White solid, (41 mg), mp 204–214 °C. Two crystallizations (2:1 EtOH/CH_2Cl_2) gave 35 mg, mp 224.5–227.5 °C, of a 6:4 mixture (by integration of the *t*-Bu signals) of 2-(3′,5′-dibromomesityl)-2-(3-bromomesityl)-1-*tert*-butylvinyl acetate and 2,2-bis(3,5-dibromomesityl)-1-*tert*-butylvinyl acetate. ^1H NMR ($CDCl_3$) δ: 1.04, 1.05 (7) (together 9 H, 2 s, *t*-Bu), 1.69, 1.71 (7) (together 3 H, 2 s, OAc), ca. 1.8 (6 H, br s), 2.04 (6 H, br s, 2 *o*-Me of 7), 2.31, 2.35 (2 br s), 2.55 (3 H, br s, *o*-Me), 2.65, 2.67 (7) (together 6 H, 2 s, *p*-Me), 2.87 (3 H, s, *o*-Me), ca. 6.8 (1 H, br m, Ar-H). Mass spectrum (125 °C, 70 eV) *m/z* (relative abundance, assignment): [696, 694, 692 (2, 3, 2, M of 7), 656, 654, 652, 650, 648 (4, 15, 23, 15, 4, M of 7 - CH_2CO)], 617, 615, 613, 611 (4, 11, 11, 4, M - H), 575, 573, 571, 569 (27, 78, 76, 27, M - Ac), 518, 516, 514, 512 (1, 3, 3, 1, M - Ac - *t*-Bu), 479, 477, 475 (6, 10, 6, M - Br - *t*-Bu), 438, 436, 434 (4, 8, 5, MH - Br - *t*-Bu - CH_2CO), 394, 392, 390 (5, 10, 5, M - Br - CH_2 - C(OAc)-*t*-Bu), 321, 319, 317 (2, 4, 2, Br_2MesC=CHOH), 119 (3, Mes), 84 (51), 57 (B, *t*-Bu), 43 (77, MeCO). Anal. Calcd for $C_{26}H_{31}Br_3O_2$: C, 50.76; H, 5.08. Calcd for 6:4 mixture of $C_{26}H_{31}Br_3O_2$ and $C_{26}H_{30}Br_4O_2$: C, 48.28; H, 4.74. Found: C, 48.76; H, 4.90.

II. White solid, (246 mg), mp 126–136 °C. Crystallization (2:1 EtOH/CH_2Cl_2) gave a mixture of the 3,3′-dibromo and 3,3′,5-tribromo derivatives according to the microanalysis, mp 148–154 °C (120 mg). ^1H NMR ($CDCl_3$) δ: 1.02, 1.04 (9 H, 2 s, *t*-Bu), 1.63, 1.66, 1.69 (3 H, 3 s, OAc), 1.84 (br m, *o*-Me), 2.06 (br s, *o*-Me), 2.31, 2.35 (6 H, 2 s, *p*-Me), 2.36 (br s, *o*-Me), 2.65, 2.67 (2 s), 2.86 (br s, *o*-Me), 6.78, 6.95 (2 H, 2 br m, Ar-H). Anal. Calcd for $C_{26}H_{32}Br_2O_2$: C, 58.23; H, 6.01. Found: C, 54.47; H, 5.55%.

III. White solid (22 mg), mp 68–79 °C. Crystallization (2:1 EtOH/CH_2Cl_2) gave 12 mg of 2,2-bis(3-bromo-2,4,6-trimethylphenyl)-1-*tert*-butylvinyl acetate, mp 144–146 °C. ^1H NMR ($CDCl_3$) δ: 1.02, 1.03 (9 H, 2 s, *t*-Bu), 1.64, 1.67 (3 H, 2 s, OAc), 1.84 (br m, *o*-Me), 2.03 (br m, *o*-Me), 2.31, 2.35 (6 H, 2 s, *p*-Me), 2.56 (br s, *o*-Me), ca. 2.7 (br m), 2.86 (br m, 2 H-3 H Mes-H). Mass spectrum (90 °C, 70 eV) *m/z* (relative abundance, assignment): 538, 536, 534 (8, 15, 8, M), 496, 494, 492 (53, 100, 52, M - CH_2CO), 416, 414 (7, 7, M - Br - CHCO), 401, 399 (4, 4, MH - Br - CH_2CO), 386, 384 (4, 4, MH - Br - Me - CH_2CO), 315, 313 (14, 14, $BrMes_2$ - 2H), 241, 239 (7, 7, $BrMesCH_2CO$), 227, 225 (4, 4, BrMesCO), 57 (73, *t*-Bu). Mass spectrum (CI, NH_3) *m/z*: 556, 554, 552 (43, 100, 40, MNH_4^+), 479, 477, 475 (4, 14, 6, M - OAc). Mass spectrum (CI, isobutane) *m/z*: 479, 477, 475 (47, 100, 38, $(BrMes)_2C$=C-*t*-Bu), 399, 397 (11, 11, $(BrMes)_2C$=C(Br)-*t*-Bu), 339, 337 (4, 3), 304 (12). Anal. Calcd for $C_{26}H_{32}Br_2O_2$: C, 58.23; H, 6.01. Found: C, 57.75; H, 6.05.

(b) 2,2-Bis(3,5-dibromomesityl)-1-*tert*-butylvinyl Acetate (7). To a stirred mixture of 6 (0.25 g, 0.7 mmol) and granular (60 mesh) iron (15 mg, 0.2 mmol) in CCl_4 (10 mL) was added dropwise bromine (0.34 mL, 6.4 mmol) in CCl_4 (9 mL) in the dark at room temperature during 1 h. HBr was evolved. The light-brown mixture was stirred for 22 h, and then $Na_2S_2O_3$ solution (5%, 2.30 mL) was added until discharge of the bromine color. Water (30 mL) and CCl_4 (30 mL) were added, the phases were separated, and the organic phase was washed with water (2 × 25 mL) and dried ($MgSO_4$). Evaporation of solvent gave a white solid (0.4 g, 89%), mp 245–247 °C. Purification is achieved either by chromatography on silica using 8:2 petroleum ether/CH_2Cl_2 eluent or by heating with EtOH and filtering the insoluble pure **7** (230 mg, 51%), mp 255 °C. IR (Nujol) ν_{max}: 1750 (C=O), 1600 (C=C) cm^{-1}. ^1H NMR ($CDCl_3$) δ: 1.05 (9 H, s, *t*-Bu), 1.71 (3 H, s, OAc), 2.01 (6 H, br s, *o*-Me), 2.62 (3 H, br s, *o*-Me), 2.65, 2.67 (6 H, 2 s, *p*-Me), 2.89 (3 H, br s, *o*-Me). Mass spectrum (200 °C, 70 eV) *m/z* (relative abundance, assignment): 698, 696, 694, 692, 690 (2, 8, 12, 8, 2, M), 656, 654, 652, 650, 648 (17, 66, 100, 68, 18, M - CH_2CO), 559, 557, 555, 553 (4, 10, 10, 4, M - CH_3 - CH_2CO - Br), 518, 516, 514, 512 (4, 10, 10, 4, M - Br - CH_2CO - Me_2C=CH_2), 494, 492, 490 (3, 6, 3, M - 2Br - CH_2CO), 320, 318, 316 (3, 7, 3, $Br_2MesCCHO$), 57 (48, *t*-Bu), 43 (53, MeCO). Anal. Calcd for $C_{26}H_{30}Br_4O_2$: C, 44.99; H, 4.36. Found: C, 45.25; H, 4.25.

When the crude material (0.4 g) was first chromatographed on a TLC plate, **3d** (37 mg, 8%) was also obtained.

1-*tert*-Butyl-2,2-bis(3,5-dibromomesityl)ethenol (**3d**). To a solution of 1-*tert*-butyl-2,2-dimesitylvinyl acetate (347 mg, 0.5 mmol) in dry THF (20 mL) was slowly added $LiAlH_4$ (38 mg, 1 mmol), and the mixture was stirred for 2 h. Water (5 drops) and then a 5% solution of aqueous NH_4Cl (10 mL) were added to the green suspension. The solid formed was filtered, extracted with warm ether (3 × 10 mL), and washed with water (2 × 10 mL), and the organic phase was dried ($MgSO_4$) and evaporated, giving white crystals of **3d** (304 mg, 93%), mp 191–4 °C. Crystallization (2:1 Et_2O/CH_2Cl_2) gave white crystals of pure **3d**, mp 196 °C. IR (Nujol) ν_{max}: 3500 (OH), 1615 (C=C) cm^{-1}. ^1H NMR ($CDCl_3$) δ: 1.09 (9 H, s, *t*-Bu), 2.29, 2.33 (2 × 6 H, 2 s, *o*-Me), 2.66, 2.68 (2 × 3 H, 2 s, *p*-Me), 4.85 (1 H, s, OH). Mass spectrum (160 °C, 70 eV) *m/z* (relative abundance, assignment): 656, 654, 652, 650, 648 (13, 49, 73, 50, 13, M), 575, 573, 571, 569 (4, 10, 11, 4, M - Br), 494, 492, 490 (6, 10, 6, M - 2Br), 394, 392, 390 (4, 7.5, 4, M - 2Br - MeCO - *t*-Bu), 321, 319, 317 (7, 14, 7, Br_2MesCO), 307, 305, 303 (4, 8, 5, Br_2MesCO), 291, 289, 287 (4, 7, 4, Br_2MesC), 57 (B, *t*-Bu). Anal. Calcd for $C_{24}H_{28}Br_4O$: C, 44.22; H, 4.33. Found: C, 44.55; H, 4.56.

Bis(3,5-dibromomesityl)methyl *tert*-Butyl Ketone (**4d**). A solution of 1-*tert*-butyl-2,2-bis(3,5-dibromomesityl)ethenol (**3d**) (32 mg, 0.046 mmol) in dry hexane (25 mL) containing CF_3COOH (0.01 mL, 0.09 mmol) was stirred at room temperature for 65 h and then refluxed for 26 h. The solvent was evaporated, and the remainder was chromatographed on a preparative silica TLC plate using 3:1 petroleum ether/CH_2Cl_2 eluent. The second fraction gave bis(3,5-dibromomesityl)methyl *tert*-butyl ketone (**4d**) (3 mg, 9.4%) as a white solid, mp 190–191 °C. IR (Nujol) ν_{max}: 1700 (C=O, s) cm^{-1}. ^1H NMR ($CDCl_3$) δ: 1.11 (9 H, s, *t*-Bu), 2.24 (12 H, s, *o*-Me), 2.71 (6 H, s, *p*-Me), 5.94 (1 H, s, CH). Mass spectrum (165 °C, 70 eV) *m/z* (relative abundance, assignment): 654, 652, 650 (0.9, 1.4, 1, M), 570, 568, 566, 564 (13, 47, 51, 48, M - H - CO-*t*-Bu), 491, 489, 487, 485 (5, 14, 14, 5, M - Br - CO - C_4H_8), 475, 473, 471, 469 (5, 13, 14, 5, M - Br - CO-*t*-Bu - Me), 394, 392, 390 (25, 48, 26, M - 2Br - CO-*t*-Bu - Me), 328, 326 (35, 35, M - 2Br - CO-*t*-Bu), 217 (29), 85 (74, CO-*t*-Bu), 57 (B, *t*-Bu). Anal. Calcd for

(29) Zipori, E.; Rappoport, Z. *Tetrahedron Lett.* **1991**, *32*, 6391.

$C_{24}H_{28}Br_4O$: C, 44.21; H, 4.33. Found: C, 44.48; H, 4.29.

Bis(pentamethylphenyl)ketene (10) was prepared by a modified Hegarty's procedure.[15] Bis(pentamethylphenyl)acetic acid (2.5 g, 7.1 mmol) was refluxed with thionyl chloride (0.7 mL) and pyridine (0.6 mL) in dry toluene (25 mL) for 20 min. The solvent was evaporated, giving the light-yellow ketene (2.02 g, 80% yield), mp 152–152.5 °C (lit.[15] 153–156 °C). IR (Nujol) ν_{max}: 2095 (C=C=O) cm^{-1}.

2,2-Bis(pentamethylphenyl)ethenol (9a). To a dark brown solution of **10** (246 mg, 0.73 mmol) in dry THF (10 mL) was slowly added $LiAlH_4$ (40 mg, 1.2 mmol). After stirring the dark-green mixture for 1 h, the unreacted $LiAlH_4$ was destroyed with water (4 drops). Anhydrous $MgSO_4$ (60 mg) was added, and the inorganic salts were filtered. Evaporation of the filtrate gave crude brown 2,2-bis(pentamethylphenyl)ethenol (205 mg), mp 125–140 °C. Addition of 3% HCl (10 mL) to the precipitate and extractions with ether (4 × 5 mL) gave an additional 12 mg of **9a**. Chromatography (dry silica column; 7:3 petroleum ether/CH_2Cl_2 eluent) gave 130 mg (60%) of **9a**, mp 169–171 °C. Crystallization (CH_2Cl_2) gave pure **9a**, as a yellowish solid, mp 187 °C. IR (Nujol) ν_{max}: 3226 (OH, m), 1625 (C=C, m) cm^{-1}. ^1H NMR ($CDCl_3$, room temperature) δ: 2.13, 2.19, 2.20, 2.24, 2.25 (30 H, 5 s, 10 Me), 4.73 (1 H, d, J = 14 Hz, OH), 6.30 (1 H, d, J = 14 Hz, CH). ^1H NMR (DMSO, room temperature) δ: 1.98, 2.10, 2.16 (30 H, 3 s, 10 Me), 6.31 (1 H, s, CH), 8.83 (1 H, s, OH). Mass spectrum (EI, 90 °C, 70 eV) m/z (relative abundance, assignment): 336 (B, M), 321 (46, M – Me), 306 (11, M – 2Me), 291 (10, M – 3Me), 276 (7, M – 4Me), 188 (14, ArCCOH), 187 (111, ArCCO), 173 (19, ArCCOH – Me), 168 (11), 145 (122, C_6Me_5 – 2H). Anal. Calcd for $C_{24}H_{32}O$: C, 85.66; H, 9.58. Found: C, 85.91; H, 9.45%.

1,1-Bis(pentamethylphenyl)propen-2-ol (9b). To a solution of ketene **10** (0.3 g, 0.9 mmol) in dry THF (10 mL) at −18 °C under argon was added dropwise a solution of 1.4 M MeLi in ether (Aldrich, 0.84 mL, 1.17 mmol). The mixture was stirred for 3 h and worked up as described above. Bis(pentamethylphenyl)acetic acid (0.12 g) was obtained from the K_2CO_3 extract. Evaporation of the solvent and chromatography on silica (96:4 petroleum ether/ether eluent) gave 190 mg of 1,1-bis(pentamethylphenyl)propen-2-ol (**9b**), mp 184.5–185.5 °C. On attempted crystallization from ether, CH_2Cl_2, $CHCl_3$, MeOH, or hexane, both the solution and the crystals develop red, pink, or violet colors. Some decomposition was observed by NMR. IR (Nujol) ν_{max}: 3499 (m, OH), 1636 (C=C, m) cm^{-1}. ^1H NMR ($CDCl_3$, room temperature) δ: 1.75 (3 H, s, Me), 2.08, 2.18, 2.23 (30 H, 3 s, 10 Me), 5.00 (1 H, s, OH). Mass spectrum (70 °C, 70 eV) m/z (relative abundance, assignment): 351 (98, M), 336 (B, M – Me), 321 (15, M – 2Me), 306 (5, M – 3Me), 291 (M – 4Me), 276 (4, M – 5Me), 187 (13, C_6Me_5CCO), 175 (C_6Me_5CO). Anal. Calcd for $C_{25}H_{34}O$: C, 85.66; H, 9.78. Found: C, 85.66; H, 9.81.

1-Mesityl-2,2-bis(pentamethylphenyl)ethenol (9c). To a stirred solution of MesMgBr (1 M in THF; 0.75 mL, 0.75 mmol) was added dropwise a solution of ketene **10** (167 mg, 0.5 mmol) during 15 min. The pink mixture was refluxed for 4 h, poured into a 5% aqueous NH_4Cl solution (20 mL), and extracted three times with ether (3 × 15 mL), and the organic phase was washed with water (2 × 10 mL), dried ($MgSO_4$), and evaporated. Chromatography of the remainder (200 mg) on a dry silica column with 3:1 petroleum ether (40–60 °C)/CH_2Cl_2 eluent gave 1-mesityl-2,2-bis(pentamethylphenyl)ethenol (**9c**) (93 mg, 41%) as a white solid. It becomes violet in air and yellow on the TLC plate but is colorless when dried under Ar. Crystallization (CH_2Cl_2) gives the solvate **9c**·CH_2Cl_2 (60 mg, 26%), mp 137 °C. IR (Nujol) ν_{max}: 3486 (OH, m), 1600 (C=C, m) cm^{-1}. ^1H NMR ($CDCl_3$) δ: 1.79 (6 H, br s, 2 Me), 1.83, 1.84 (6 H, 2 s, 2 Me), 1.93, 2.05 (2 × 3 H, 2 s, Me), 2.13, 2.14 (6 H, 2 s, 2 Me), 2.20, 2.26, 2.29, 2.44, 2.56 (5 × 3 H, 5 s, 5 Me), 5.30 (2 H, s, CH_2Cl_2), 5.31 (1 H, s, OH), 6.55, 6.86 (2 H, 2 s, Mes-H). Mass spectrum (110 °C, 70 eV) m/z (relative abundance, assignment): 455 (44, M), 440 (14, M – Me), 423 (6, M – 2Me), 147 (17, MesCO), 132 (59, MesCH), 119 (15, Mes), 117 (61, Mes – H_2), 116 (78, Mes – 3H), 105 (32, $C_6H_3Me_2$), 91 (18, C_7H_7), 18 (B, H_2O).

Also eluted from the column was **9a** (15 mg, 9%), mp 187–188 °C and a second compound (2 mg) which was not identified.

1,1-Bis(pentamethylphenyl)-3,3-dimethyl-1-buten-2-ol (9d). To a dark-brown solution of ketene **10** (0.6 g, 1.8 mmol) in dry ether (20 mL) at −40 °C under Ar was added dropwise during 10 min a solution of 1.7 M t-BuLi in pentane (1.4 mL, 2.4 mmol), the mixture was stirred for an additional 3 h, and the dark-red solution was worked up as described above. Evaporation of the solvent gave a yellow-beige precipitate (0.65 g), mp 156–170 °C. Bis(pentamethylphenyl)acetic acid (0.25 g) was obtained from the K_2CO_3 extract. Chromatography on silica (9:1 petroleum ether (40–60 °C)/ether eluent) gave 290 mg of **9d**. Crystallization (ether/CH_2Cl_2) under argon gave pink to red crystals. Crystallization from hexane gave colorless crystals, mp 196–197 °C. IR (Nujol) ν_{max}: 3518 (OH, m), 1600 (C=C, m) cm^{-1}. ^1H NMR ($CDCl_3$) δ: 1.08 (9 H, s, t-Bu), 2.11, 2.13, 2.14, 2.15, 2.19, 2.20 (30 H, 6 s, Me), 4.91 (1 H, s, OH). ^1H NMR (DMSO-d_6, room temperature) δ: 0.99 (9 H, s, t-Bu), 2.00, 2.06, 2.12 (30 H, 3 s, Me), 6.91 (1 H, s, OH). Mass spectrum (50 °C, 70 eV) m/z (relative abundance, assignment): 392 (45, M), 377 (11, M – Me), 362 (2, M – 2Me), 347 (3, M – 3Me), 119 (3, Mes), 57 (38, t-Bu), 18 (B, H_2O). Anal. Calcd for $C_{28}H_{40}O$: C, 85.66; H, 10.27. Found: C, 85.92; H, 10.26.

1,1-Bis(pentamethylphenyl)-2-propanone (11b). 1,1-Bis(pentamethylphenyl)-1-propen-2-ol (**9b**) (130 mg, 0.37 mmol) and CF_3COOH (2 drops) in hexane (25 mL) were kept in an ampule for 8 h at 80 °C. The solvent was evaporated, and chromatography of the remainder (silica, 9:1 petroleum ether/ether eluent) gave enol **9b** (14 mg) and ketone **11b** (26 mg). Crystallization (hexane) gave light-yellow crystals of 1,1-bis(pentamethylphenyl)-2-propanone (**11b**), mp 156 °C. IR (Nujol) ν_{max}: 1696 cm^{-1} (C=O, s). ^1H NMR ($CDCl_3$) δ: 1.25 (3 H, s, α-Me), 2.01, 2.19 (2 × 12 H, 2 s, o- + m-Me), 2.24 (6 H, s, p-Me), 5.52 (1 H, s, CH). Mass spectrum (EI, 70 eV) m/z (relative abundance, assignment): 351 (10, M), 308 (B, $(Me_5C_6)_2CH^+$), 135 (5, MesO), 119 (2, Mes). Anal. Calcd for $C_{25}H_{34}O$: C, 85.66; H, 9.78. Found: C, 85.98; H, 10.00.

1,1-Bis(pentamethylphenyl)-3,3-dimethyl-2-butanone (11c). 1,1-Bis(pentamethylphenyl)-3,3-dimethyl-1-buten-2-ol (**9d**) (13 mg, 0.03 mmol) and CF_3COOH (2 drops) in hexane (25 mL) were kept in an ampule for 5 h at 80 °C. The solvent was evaporated, and chromatography (preparative TLC silica plate, 65% petroleum ether/35% CH_2Cl_2 eluent) gave ketone **11c** (10 mg, 77%) as yellowish plates, mp 172–174 °C. IR (Nujol) ν_{max}: 1699 (C=O, m) cm^{-1}. ^1H NMR ($CDCl_3$) δ: 1.03 (9 H, s, t-Bu), 2.02, 2.17 (2 s, 2 × 12 H, o- + m-Me), 2.24 (6 H, s, p-Me), 5.94 (1 H, s, CH). Mass spectrum (EI, 100 °C, 70 eV) m/z (relative abundance, assignment): 307 (B, $(Me_5C_6)_2CH^+$), 262 (7, $(Me_5C_6)_2CH$ – 3Me), 175 (11, C_6Me_5CO), 135 (18, $C_7H_6Me_3$ or MesO), 119 (8, Mes), 97 (13), 57 (57, t-Bu). Mass spectrum (CI, isobutane) m/z (relative abundance, assignment): 392 (3.3, M), 308 (8, MH – CO-t-Bu), 263 (9.8), 245 (B, $Me_5C_6CH_2CO$-t-Bu). Anal. Calcd for $C_{28}H_{40}O$: C, 85.66; H, 10.27. Found: C, 85.39; H, 10.50.

Equilibration Studies. The 9 ⇌ 11 System. Enols **9a,c,d** and ketones **11b** and **11c** were equilibrated by the following procedure. An ampule containing the enol (11 mg) in spectroscopic hexane (10 or 25 mL) to which CF_3COOH (0.1 mL, 0.001 mM) was added was kept at 80 ± 1 °C. The ampule was opened, the solvent was evaporated during 4 h, and TLC and ^1H NMR ($CDCl_3$) were recorded. The sample was diluted with hexane/TFA, and the reaction continued. Only with **9a**, several independent ampules were used. Specific comments are as follows.

9a: After 10, 36, and 75 h, at 80 °C the solutions were light blue, blue, and gray, respectively. The percentage of **11a** was calculated from the relative integration of the expanded CH signals of **11a** at δ 6.29. The error is relatively large, since the percentage of **11a** is only ca. 0.5%.

9b: On addition of the TFA at room temperature, the solution becomes successively cherry red, pink, and yellow after a few seconds and, after solvent evaporation, it is brown-green. After 4.5 h the TLC shows two strong spots ascribed to **9b** and **11b** and two weak spots ascribed to decomposition products. NMR ($CDCl_3$) δ: 1.26 (Me, **11b**), 1.75 (**9b**) (3 H together, 2 s, Me), 2.01 (**11b**), 2.08 (**9b**), 2.17, 2.18 (**9b**), 2.19 (**11b**), 2.23, 2.234 (**9b**), 2.24 (**11b**) (30 H together, 8 s, 10 Me), 4.99 (OH, **9b**), 5.52 (CH, **11b**) (1 H together, 2 s). After 12 and 60 h, additional weak signals at δ ($CDCl_3$) 1.93, 2.11, 2.13, 2.25, 2.28, 2.30, and 2.47 were observed.

Integration of the methyl signals of **9b** and **11b** gave their relative ratio. Sometimes the relative integration ratio of δ(CH-**11b**)/δ(OH-**9b**) was an additional probe. However, exchange of the enolic OH with traces of TFA complicated the integration. Correction of the δ 2.08/δ 2.01 ratio was needed after 60 h due to appearance of a small decomposition signal.

11b: After 8 h at 80 °C the solution was yellow-brown and TLC and ^1H NMR showed the same pattern as from **9b**. Equilibrium data are in Table VIII.

9d: On addition of TFA (0.03 mL, 0.27 mmol) to **9d** at room temperature, the solution immediately turns light cherry red and after a few minutes to lemon yellow. Such color change is not observed when the TFA is added under argon. The solution turns green or lemon yellow on heating. After 60 h TLC shows spots for **11c** and **9d** and weak "decomposition" spots. After 5 h ^1H NMR ($CDCl_3$) shows δ: 1.03 (**11c**), 1.08 (**9d**) (together 9 H, 2 s, t-Bu), 2.02 (**11c**), 2.11, 2.13, 2.14, 2.16 (**9d**, o- + m-Me), 2.17 (**11c**), 2.196, 2.204 (**9d**, p-Me), 2.24 (**11c**) (together 30 H, 9 s, 10 Me), 4.91 (**9d**, s, OH), 5.94 (**11c**, s, CH) (together 1 H). The **9d**/**11c** ratios were determined by integration of the t-Bu signals and sometimes also of the δ(OH-**9d**)/δ(CH-**11c**) signals.

11c: The solution turns green on heating, giving a yellow-brown solid. After 5 h of heating, the ^1H NMR ($CDCl_3$) resembled that described for **9d** above. After longer reaction time, decomposition signals were

observed. Data are given in Table VIII.

Attempted Equilibration of Enols 3b and 3d. (a) A solution of enol **3b** (20 mg, 0.033 mmol) in dry hexane (25 mL) containing CF_3COOH (1 drop) was refluxed for 72 h. TLC showed no product and after evaporation of the solvent **3b** was recovered. (b) The isomerization experiment starting from **3d** (32 mg) was described above. After reflux for 26 h, **4d** (9.4%) was isolated, and from the chromatography, **3d** (77 mg, 53%) was recovered.

Attempted Enolization of Bis(3-bromo-2,4,6-trimethylphenyl)methyl *tert*-Butyl Ketone. The ketone (18 mg, 0.036 mmol) was dissolved in spectroscopic hexane (10 mL) containing TFA (0.1 mL, 0.001 mmol) and kept at 80 °C. Even after 309 h when TLC showed the presence of six new weak spots, the main spot was that of the ketone and the NMR was identical to that of the ketone. Consequently, no enolization took place.

Crystallographic Parameters. 3a: $C_{20}H_{20}Br_4O\cdot Et_2O$, M = 670.1, space group C_2/c, a = 33.00 (1) Å, b = 9.151 (4) Å, c = 18.442 (4) Å, β = 112.71 (5)°, V = 5137 (1) Å^3, Z = 8, ρ_{calcd} = 1.73 g cm^{-3}, $\mu(CuK_\alpha)$ = 73.2 cm^{-1}, no. of unique reflections = 3671, no. of reflections with $I \geq 3\sigma_I$ = 3176, R = 0.066, R_w = 0.120, $w^{-1} = \sigma F^2 + 0.006\,836F^2$. **3b**: $C_{21}H_{22}Br_4O\cdot Et_2O$, M = 684.1, space group $P2_1/c$, a = 12.656 (4) Å, b = 10.670 (3) Å, c = 20.684 (5) Å, β = 104.38 (3)°, V = 2705.7 (8) Å^3, Z = 4, ρ_{calcd} = 1.68 g cm^{-3}, $\mu(MoK_\alpha)$ = 58.35 cm^{-1}, no. of unique reflections = 4505, no. of reflections with $I \geq 3\sigma_I$ = 1937, R = 0.070, R_w = 0.077, $w = \sigma F^{-2}$. **3c**: $C_{29}H_{30}Br_4O\cdot MeOH$, M = 746.2, space group $P\bar{1}$, a = 12.935 (5) Å, b = 14.194 (6) Å, c = 9.286 (4) Å, α = 97.96 (2)°, β = 95.38 (2)°, γ = 63.39 (2)°, V = 1508.4 (2) Å^3, Z = 2, ρ_{calcd} = 1.64 g cm^{-3}, $\mu(MoK_\alpha)$ = 52.37 cm^{-1}, no. of unique reflections = 3769, no. of reflections with $I \geq 2\sigma_I$ = 2325, T = 0.066, R_w = 0.067, $w = (\sigma F^2 + 0.000\,139F^2)^{-1}$. **3d**: $C_{24}H_{28}Br_4O$; M = 652.1, space group $P2_1/n$, a = 21.146 Å, b = 12.869 Å, c = 8.944 Å, β = 93.16°, V = 2430.2 Å^3, Z = 4, ρ_{calcd} = 1.78 g cm^{-3}, $\mu(MoK_\alpha)$ = 64.92 cm^{-1}, no. of unique reflections = 3538, no. of reflections with $I \geq 3\sigma_I$ = 2249, R = 0.056, R_w = 0.076, $w^{-1} = \sigma F^2 + 0.004\,657F^2$. **9a**: $C_{24}H_{32}O \cdot 0.5\ CH_2Cl_2$, M = 419.0, space group $P\bar{1}$, a = 13.152 (2) Å, b = 14.522 (2) Å, c = 12.624 (2) Å, α = 112.31 (2)°, β = 97.49 (2)°, γ = 92.59 (2)°, V = 2199.8 (7) Å^3, Z = 4, ρ_{calcd} = 1.14 g cm^{-3}, $\mu(CuK_\alpha)$ = 16.01 cm^{-1}, no. of unique reflections = 5521, no. of reflections with $I \geq 3\sigma_I$ = 4733, R = 0.069, R_w = 0.127. **9d**: $C_{28}H_{40}O$, M = 392.6, space group $P2_1/n$, a = 21.031 (5) Å, b = 12.862 (3) Å, c = 8.762 (3) Å, β = 93.65 (2)°, V = 2365.3 (9) Å^3, Z = 4, ρ_{calcd} = 1.10 g cm^{-3}, $\mu(CuK_\alpha)$ = 4.52 cm^{-1}, no. of unique reflections = 3121, no. of reflections with $I \geq 3\sigma_I$ = 2530, R = 0.070, R_w = 0.116.

X-ray Crystal Structure Analysis. Data were measured on a PW1100/20 Philips Four-Circle Computer-Controlled Diffractometer and on an ENRAF-NONIUS CAD-4 automatic diffractometer for **9**. The method and the calculations[30] (using the SHELXS-86 analysis[30a]) are identical to those described previously.[7b]

Acknowledgment. This work was supported by a grant from the United States-Israel Binational Science Foundation (BSF), Jerusalem, to which we are indebted. I.E. thanks the Absorption Ministry and J.F. thanks the A. Gal Memorial Fund for support. We are indebted to Mr. Michael Gozin for preliminary studies, to Dr. Shmuel Cohen for the X-ray crystallography, to Dr. M. Kaftory for data from the CSDB, and to the Mass Spectrometry Center at the Technion, Haifa, for several mass spectral determinations.

Supplementary Material Available: Tables S1-S30 giving bond lengths, bond angles, and positional, thermal, and structural parameters for **3a-d**, **9a**, and **9d** and Figures S1-S9 giving the ORTEP drawings of **3a-c** and **9a**, stereoscopic views of **3a**, **3b**, **3d**, and **9d**, and the unit cell of **3a** (56 pages); listing of observed and calculated structure factors for **3a-d**, **9a**, and **9d** (106 pages). Ordering information is given on any current masthead page.

(30) (a) Sheldrick, G. M. *Crystallographic Computing 3*; Oxford University Press: Oxford, U.K., 1985; pp 175-189. (b) All crystallographic computing for **3** was done on a CYBER 855 computer and for **9** on a VAX VMS computer at the Hebrew University of Jerusalem, using the SHELX 1977 Structure Determination Package for **3** and the TEXAN structure analysis software for **9**.

Aldol Additions of Pinacolone Lithium Enolate with Ketones: Reactivities Governed Predominantly by Field Effects

Goutam Das and Edward R. Thornton*

Contribution from the Department of Chemistry, University of Pennsylvania, Philadelphia, Pennsylvania 19104-6323. *Received July 15, 1992*

Abstract: The relative reactivities of representative α- and β-heterosubstituted acyclic, cyclic (five- and six-membered), and aromatic ketones with the lithium enolate of pinacolone in diethyl ether at -78 °C were determined. The order of reactivities of monosubstituted acetones ($MeCOCH_2X$) is X = Cl > OTBDMS > OMe > SMe > NMe_2 > CH_2SMe > H > Me and spans a range of 10^4. Excellent correlation was obtained for $MeCOCH_2X$ when log (k_X/k_{Me}) was plotted against $\sigma_I(X)$ (r = 0.996, ρ = 6.62), demonstrating the overwhelming importance of substituent field/inductive effects in the rate enhancement. Similar linear relationships were also observed for aromatic ketones (r = 0.993, ρ = 7.61) as well as five-membered (r = 0.997, ρ = 6.87) and six-membered ring (r = 0.998, ρ = 6.92) cyclic ketones. Thiacyclopentanone and 3- and 4-thiacyclohexanones were unique among the substrates studied in departing significantly from the correlations shown by all other types of substrates. Similarities of the reactivities for 3-oxacyclohexanone vs cyclohexanone and of 3-oxacyclopentanone vs cyclopentanone to that for methoxyacetone vs butanone established that chelation has no role in the very large rate enhancements observed. The synthetic utility of this effect for regioselective additions was demonstrated by the exclusive addition of pinacolone lithium enolate to the 2-carbonyl in $MeCO(CH_2)_3COCH_2OSiMe_2t$-Bu. Steric retardation by α-methyl and α-methoxy groups was nearly absent in cyclopentanones, small in acyclic ketones, and considerable in cyclohexanones.

Introduction

In sharp contrast to Grignard and organotitanium reagents, the stereochemical results for aldol additions of lithium[1,2] and titanium[3,4] enolates to α- and β-alkoxy aldehydes and ketones indicated that Felkin-Anh transition structures were preferred over chelated ones.[5] The determining factors are not understood, and their elucidation requires knowledge of reactivities. Useful synthetic consequences might well emerge from such studies.

(1) Heathcock, C. H.; Young, S. D.; Hagen, J. P.; Pirrung, M. C.; White, C. T.; VanDerveer, D. *J. Org. Chem.* **1980**, *45*, 3846-3856.
(2) Lodge, E. P.; Heathcock, C. H. *J. Am. Chem. Soc.* **1987**, *109*, 3353-3361.
(3) Bonner, M. P.; Thornton, E. R. *J. Am. Chem. Soc.* **1991**, *113*, 1299-1308.
(4) Reetz, M. T.; Hüllmann, M. *J. Chem. Soc., Chem. Commun.* **1986**, 1600-1602.
(5) Eliel, E. L. In *Asymmetric Synthesis*; Morrison, J. D., Ed.; Academic Press: New York, 1983; Vol. 2, pp 125-155.

0002-7863/93/1515-1302$04.00/0